Review

Human-Mouse Convergence in Metabolic Dysfunction-Associated Steatotic Liver Disease: Mouse Model Selection and Non-Invasive Diagnostic Strategies

Denise Bonente [†], Sara Gargiulo [†], Ludovica Livi, Matteo Gramanzini, Tiziana Tamborrino, Lisa Gherardini, Giovanni Inzalaco, Lorenzo Franci, Mario Chiariello, Virginia Barone [*]

Posted Date: 24 February 2026

doi: 10.20944/preprints202602.1274.v1

Keywords: metabolic dysfunction-associated steatotic liver disease; non-alcoholic fatty liver disease; MASLD; hepatic steatosis; mouse models; non-invasive imaging

 doi:10.20944/preprints202602.1274.v1

Review

Human-Mouse Convergence in Metabolic Dysfunction-Associated Steatotic Liver Disease: Mouse Model Selection and Non-Invasive Diagnostic Strategies

Denise Bonente [1,2,†], Sara Gargiulo [3,†], Ludovica Livi [4], Matteo Gramanzini [5], Tiziana Tamborrino [1,2], Lisa Gherardini [3], Giovanni Inzalaco [6], Lorenzo Franci [7], Mario Chiariello [3,8] and Virginia Barone [1,*]

[1] Department of Molecular and Developmental Medicine, University of Siena, 53100 Siena, Italy
[2] Department of Life Sciences, University of Siena, 53100 Siena, Italy
[3] Institute of Clinical Physiology, National Research Council, Via Fiorentina 1, 53100 Siena, Italy
[4] Department of Medical, Surgical and Neurological Science, University of Siena, 53100 Siena, Italy
[5] Institute of Crystallography, National Research Council, Montelibretti Division, Strada Provinciale 35d, 9-00010 Rome, Italy
[6] Institute of Endotypes in Oncology, Metabolism and Immunology "Gaetano Salvatore", National Research Council, Via Pansini 5, 80131, Napoli, Italy
[7] Department of Industrial Chemistry "Toso Montanari", University of Bologna, Bologna 40136, Italy
[8] Core Research Laboratory, Istituto per lo Studio, la Prevenzione e la Rete Oncologica, 53100, Siena, Italy
* Correspondence: virginia.barone@unisi.it; Tel.: +39 0577 232053
† These authors contributed equally to this work.

Abstract

Background Metabolic Dysfunction-Associated Steatotic Liver Disease (MASLD) is a global health priority affecting approximately 30% of the population. It represents the hepatic manifestation of metabolic syndrome, potentially progressing from simple steatosis to Metabolic Dysfunction-Associated Steatohepatitis (MASH), cirrhosis, and hepatocellular carcinoma. This review aims to compare current knowledge of MASLD in mouse models and humans, focusing on pathophysiology, histological phenotypes, and the role of preclinical imaging as a non-invasive translational screening tool. **Methods** The study synthesizes recent evidence (last five years) regarding the multifactorial aetiology of MASLD, focusing on some of the key aspects in selecting the appropriate animal model and on the recent non-invasive techniques applicable to both humans and mice. **Results** MASLD arises from complex interactions between genetics, sedentary lifestyles, and imbalanced diets. While mouse models have been refined to capture the multifactorial interplay driving disease progression and are still essential for drug development, no single model fully mirrors the human condition. This process must take into account key variables, including diet composition, mouse strain, the use of genetically modified mice (GEMs), and housing temperature. Histological assessment remains the gold standard for MASLD staging, particularly in mouse models; however, preclinical imaging is increasingly emerging as a complementary, non-invasive technique for in vivo investigation. **Conclusions** Rational, fit-for-purpose mouse models are essential to address specific mechanistic and therapeutic questions. Given the multifactorial and heterogeneous nature of MASLD, understanding the limitations and strengths of specific mouse models is therefore crucial for translational research. Integrating phenotype-driven approaches in both humans and mice, combining traditional histology, quantitative imaging and metabolic profiling, as well as longitudinal, combinatorial and humanized preclinical models, will enhance translational alignment and accelerate the development of therapies for MASLD.

 doi:10.20944/preprints202602.1274.v1

Keywords: metabolic dysfunction-associated steatotic liver disease; non-alcoholic fatty liver disease; MASLD; hepatic steatosis; mouse models; non-invasive imaging

1. Hepatic Steatosis and Metabolic Dysfunction-Associated Steatotic Liver Disease (MASLD): Overview

Hepatic steatosis is defined as the presence of intrahepatic fat, accounting for at least 5% of total liver weight [1]. It can be caused by excessive alcohol consumption or by metabolic factors like obesity, insulin resistance (IR) and dyslipidemia. This second condition, named Metabolic Dysfunction-Associated Steatotic Liver Disease (MASLD, previously known as Non-Alcoholic Fatty Liver Disease - NAFLD), has gained much attention in recent years due to its potential to progress to more severe forms [2]. MASLD is considered the hepatic manifestation of metabolic syndrome encompassing a spectrum of conditions that can progress from a simple, less harmful form of hepatic fat deposition to a more severe form of steatohepatitis with inflammation, iron deposition, and potential damage and fibrosis (Metabolic Dysfunction-Associated Steatohepatitis - MASH), ultimately leading to cirrhosis and hepatocellular carcinoma (HCC) [3,4].

Its global prevalence is very high, affecting approximately 30% of the population, and its incidence has increased by 50.4% from 1990 to the present [5]. In MASLD, hepatic steatosis is associated with at least one cardiometabolic risk factor, including hyperlipidemia, hyperglycemia, IR, and overweight [2]. Although MASLD has been considered, for many years, a condition closely linked to obesity, increasing evidence shows that it can develop also in individuals with a normal body mass index (BMI), a condition known as “lean-MASLD” [6]. Indeed, MASLD is a multifactorial disease whose pathophysiology is not yet fully understood, arising from a combination of genetic predisposition, dietary factors, physical activity levels, and gut dysbiosis [7].

Genetic factors play a significant role in MASLD, with variants identified in genes that regulate glucose and fat regulatory pathways. For example, the rs738409 (c.444C>G) polymorphism in the patatin-like phospholipase domain-containing 3 (PNPLA3) gene is present in 30–50% of individuals with MASLD. This variant leads to an isoleucine-to-methionine substitution at position 148 (p.I148M), resulting in increased hepatic lipid retention during feeding and excessive lipid oxidation during fasting. These alterations overwhelm metabolic capacity and ultimately promote cellular toxicity, leading to hepatic damage [8]. Another well-known polymorphism is the HSD17B13 variant of 17β-hydroxysteroid dehydrogenase-13, which is a hepatocyte-specific, lipid droplet-associated protein. HSD17B13 gene expression and protein levels are upregulated in MASLD affected patients and overexpression of Hsd17b13 in mice promotes rapid lipid accumulation in the liver [9]. Also, the missense variant rs1260326 (p.P446L) and the intronic variant rs780094 of Glucokinase regulatory protein gene (GCRK) are associated with increased de novo lipogenesis and higher plasma triglycerides levels [10]. Single-nucleotide polymorphisms in membrane-bound O-acyltransferase domain–containing 7 (MBOAT7) are associated with increased risk of initiation and progression of MASLD and fibrosis; indeed multiple in vitro and in vivo studies showed how MBOAT7 deficiency in mice and humans alters the hepatic phospholipids composition and promotes hyperinsulinemia and hepatic IR [11]. Lastly, the rs58542926 variant in TM6SF2 gene (p.E167K), by inhibiting the secretion of Very Low-Density Lipoproteins from hepatocytes, promotes triglycerides accumulation within the liver parenchyma [12].

An imbalanced diet is another risk factor for MASLD. This involves alterations in both macro- and micronutrients intake, characterized not only by increased consumption of calories, i.e., carbohydrates, cholesterol, and total saturated fatty acids, but also by excessive selenium and reduced vitamins K and E intakes. Such dietary patterns promote IR and hepatic lipid accumulation, and a positive correlation has been observed between circulating selenium levels and liver fibrosis. Conversely, deficiencies in vitamins E and K contribute to increased oxidative stress and impaired glycemic control [13].

 doi:10.20944/preprints202602.1274.v1

Alongside imbalanced dietary habits, individuals with MASLD tend to be more sedentary and less likely to engage in regular physical activity [13]. Such reduced activity is clinically relevant, as exercise has been shown to be effective in preventing the onset of MASLD. Indeed, emerging evidence supports the existence of a muscle–liver crosstalk, whereby myokines released by muscles during physical activity, such as decorin and IL-6, promote mitochondrial fatty acid β-oxidation, mitigating diet-induced hepatic steatosis and attenuating hepatic inflammation [14,15].

Regarding gut dysbiosis, patients with MASLD frequently exhibit an imbalanced gut microbiota, characterized by an overrepresentation of Proteobacteria and Fusobacteria, phyla that include many opportunistic pathogens, and a concomitant reduction in protective genera such as *Prevotella* and *Faecalibacterium*. This could compromise gut barrier integrity and the production of short-chain fatty acids, leading to gut leakiness and chronic inflammation [16].

Given its multifactorial etiology, MASLD remains a therapeutic challenge. Current management strategies primarily focus on dietary modifications, increased physical activity, and pharmacological interventions with drugs such as Pioglitazone, Vitamin E, and antagonists of the glucagon-like peptide-receptor 1 (GLP-1R) and peroxisome proliferator–activated receptor (PPAR) [17]. In this context, experimental mouse models of MASLD play a fundamental role, as they enable detailed investigation of the disease's pathophysiology and may help uncover new pathways that could serve as therapeutic targets. Moreover, mouse strains have diverse genetic backgrounds and are susceptible to genetic manipulation, which helps to identify the genetic factors underlying MASLD. Compared to animal models with more developed brain functions, mice can model varying degrees of MASLD based on environmental, genetic, and epigenetic factors or their combination, with ease of management, shorter investigation times, lower costs, and fewer ethical concerns.

In both humans and mice, MASLD is currently confirmed and staged by histology as the gold standard; however, non-invasive diagnostic and imaging approaches are increasingly recommended. In the clinical setting, recent advances in imaging enable safer image-guided liver biopsies and support integrated MASLD screening strategies for early diagnosis in high-risk patients or when biopsy is contraindicated due to underlying health conditions [18,19]. In the preclinical setting, histological assessment of MASLD requires animal sacrifice, thereby precluding longitudinal evaluation of disease progression or therapeutic response within the same subject and increasing the number of animals used at multiple experimental time points [20]. Therefore, the implementation of preclinical imaging approaches is highly relevant and translationally valuable for MASLD research, as it complements invasive methods while addressing both scientific and ethical considerations.

Considering these aspects, our aim is to critically summarize the most recent refinements of genetic and/or dietary MASLD mouse models in the last five-year publications, highlighting the varied and controversial efforts to reproduce the full spectrum of MASLD outcomes, including metabolic alterations, hepatic inflammation and fibrosis. We examined their comparability to humans and translational relevance, with a focus on current histopathological evidence for MASLD/MASH in mouse models and the advances of preclinical imaging, highlighting the key factors to consider when selecting the most appropriate animal model.

2. Mouse Models of MASLD: Strength and Pitfalls in Comparative Pathology

Currently, given the complexity of the pathophysiology of MASLD and interspecies differences in liver biology, neither cellular systems nor animal models can completely reproduce the human disease. Despite advances, both simpler 2D human cell cultures, such as HepG2 and Huh7, and human-based 3D organoids are still unable to fully reflect the complexity of hepatocytes metabolism compared to living organisms [21–24]. On the other hand, laboratory mice, the most widely used animal models for MASLD, have liver anatomy similar to humans, but also show pathophysiological differences, such as in transcriptome and enzymatic activities [25,26].

Through the years, several mouse models have been developed to study the pathogenesis and treatment of MASLD and over the past decades, extensive reviews have described the most well-established models, including diet-induced, gene editing-induced, and chemical-induced models.

 doi:10.20944/preprints202602.1274.v1

Various dietary regimens, such as high fat (HFD), methionine and/or choline deficient (MCD), cafeteria and western (WD) diets, or chemicals such as carbon tetrachloride, streptozocin or exposure to cigarette smoke, have been extensively tested in different settings on mouse strains susceptible to metabolic syndrome (C57BL/6, FVB/N, DBA/2J, 129S1/SvlmJ) or genetically engineered mouse (GEM) models including ob/ob, db/db, LDLR-/-, ApoE-/- or knock-out (KO) mice for the targeted genes of interest [27–31]. Despite this, there is still the need for further refinement to bridge the translational gap and better capture the complex interplay among genetic, metabolic, and environmental factors driving disease development and progression. In this context, models representing both early and advanced stages of MASLD are valuable for distinct and complementary research purposes. Early-stage models help to study etiopathogenesis and test preventive strategies for simple steatosis in a still reversible pathological state, and are particularly valuable as recent evidence from the LITMUS consortium has highlighted that early-stage MASLD is often underdiagnosed; conversely late-stage models are essential to study the transition to more severe consequences such as inflammation, fibrosis and cancer [32,33].

Therefore, selecting the most suitable MASLD model requires a balance between a model's ability to address a particular experimental question and its limitations in representing the full spectrum of human MASLD. Moreover, several factors must be considered, including diet selection, mouse strains, the use or not of GEM mouse model, the choice of inbred mice, and housing conditions (Figure 1).

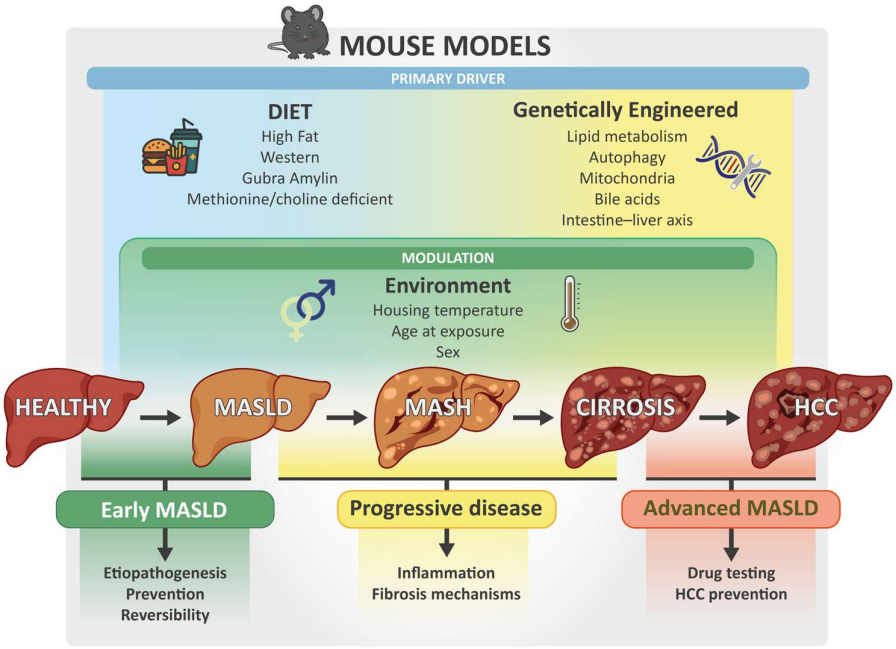

Figure 1. Mouse models: drivers, disease stages, and translational studies. The figure provides a visual framework to understand how murine models can reproduce different phases of MASLD. The central axis represents disease progression from healthy to steatotic liver, followed by the worsening of the condition to MASH, cirrosis, and HCC. Above the axis, the main experimental drivers are depicted: dietary regimens primarily determine disease progression, while genetic background and engineered models modulate key pathways such as lipid metabolism, autophagy, mitochondrial function, bile acid regulation, and gut–liver interactions. Environmental factors (housing temperature, age, and sex) further influence disease severity and kinetics. Below the spectrum, the figure links disease stages to their typical experimental use, from studies on etiopathogenesis and prevention in early MASLD to investigations of inflammation, fibrosis, and therapeutic testing in advanced stages.

Considering dietary regimens it is important to highlight that variations in diet composition and its duration can strongly influence the clinically relevant endpoints provided by mouse models;

 doi:10.20944/preprints202602.1274.v1

besides, a diet markedly different from human dietary patterns is likely to result in poorly translatable results [34].

MCD has been used in the past because it induces steatohepatitis and liver fibrosis rapidly, but its current use is limited as it does not mimic a realistic diet and the key metabolic changes of human MASLD, particularly obesity and IR. Furthermore, mice fed MCD show marked weight loss, raising both scientific and ethical concerns. For this reason, MCD models may be more suitable in specific contexts, such as to study histological aspects of liver fibrosis and inflammation and test new targeted drugs, or to investigate altered drug disposition due to MASH-associated transporter alterations [28,35,36].

Regarding diets, WD-fed mouse models are the ones that better recapitulate obesity, hypercholesterolemia, IR and histological hallmarks of human disease progression and are best suited for testing therapies to promote weight loss and ameliorate inflammation [32,37]. Indeed, WDs, with variable macronutrient compositions and feeding durations, induce a spectrum of alterations that goes from simple steatosis to MASH at 12–16, 20–24, and up to 9–18 months of age, depending on mouse genetics [31,38,39]. This diet triggers early, long-lasting disturbances, including markers of oxidative stress and mitochondrial dysfunction but also hepatic iron deposition and lipid peroxidation, characteristics of MASLD progression also in human disease [39–42]. Notably, after WD feeding, different liver lobes in mice exhibit metabolic heterogeneity similar to humans: in 8-week-old C57BL/6J mice, the left lobe showed the earliest and most severe metabolic and inflammatory changes, which progressed further after 16 weeks [42]. Combining WD with drinking water supplemented with fructose, but not glucose and sucrose, exacerbated the progression of MASLD in male C57BL/6N mice after 10 weeks, as reported in humans consuming sugar-sweetened beverages [43,44]. However, the distinct effects of various types of sugars on the progression of MASLD are still a matter of debate, and 6 weeks-old C57BL/6J mice which consumed WD containing ~ 30% fat and 20% sucrose for 24 weeks, supplemented with 30% fructose or sucrose in drinking water, showed comparable worsening of liver damage [45]. In any case, WD models are advantageous from a translational perspective because the disease is not driven by nutritional deficiencies, unusual additives, hepatotoxins, or extremely high fat content (45–69%) [32,37].

Another dietary approach that is now gaining more and more consideration is the Gubra Amylin diet (GAN) for non-alcoholic steatohepatitis , rich in fructose, saturated fat, and with 2% cholesterol [29]. This diet was able to induce hepatic steatosis and mild inflammation as early as 10 weeks of feeding in adult male C57BL/6J mice associated with colonic microbiota dysbiosis, an important cofactor in the development of MASLD in humans [46]. It may be argued that this level of cholesterol is excessive (in particular when compared to 0.2% cholesterol of WD) and does not accurately reflect the dietary intake of Western populations; on the other hand, the clinical translatability of a C57BL/6J mouse model with the same cholesterol concentration, with 40% of saturated fat (mainly palm oil) and 20% fructose for up to 44 weeks, was supported under normal housing conditions[47–50]. Indeed, these mice showed clinical features, metabolic parameters and histological alterations (macrovesicular steatosis, hepatocyte ballooning, inflammation and fibrosis) consistent with human patients, highlighting their suitability for studying therapeutic targets for MASH, even with the disadvantage of long and expensive disease induction times. MASH and fibrosis can develop more rapidly and severely by feeding this diet to GEMs [29].

In this context, beyond diet, it is also essential to consider duration of the dietary regimen and the age at which it is initiated: prolonged exposure to imbalanced diets induces the most severe alterations, closely resembling human disease, but at higher time and economic costs. In parallel, WD-fed mice display different severity of MASLD from preadolescence (20-30 days) or puberty (8 weeks) to mature adulthood (12 weeks), or until middle age (~ 15 months) and senescence (~ 20 months) [31,38,39,51,52]. Noteworthy, also GAN diet seems to induce differential progression of MASH and fibrosis at different ages. 14-months-old C57BL/6J mice fed GAN diet for 21 weeks developed severe pathological features of MASLD, comparable to those of humans, more rapidly than young mice [53]. Interestingly, the presence of macrovesicular steatosis and monocyte-derived

 doi:10.20944/preprints202602.1274.v1

macrophages, Kupffer and T cells was detected in the liver of aged male mice within 12 weeks of dietary challenge, but MASH and fibrosis progression was evident in both female and male aged mice after 21 weeks of GAN [53].

Furthermore, this mouse model has been shown to develop HCC after approximately 60 weeks of GAN diet feeding and has been useful for thoroughly characterizing therapies with lanifibranor and semaglutide, demonstrating that the latter is able to act both on the advanced stage of MASH and reduce cancer development [54].

As previously mentioned, the choice of mouse strain is of great significance, showing large differences based on the combination of dietary regimens and genetic background [55]. A further challenge concerns the choice of inbred animals: their low genetic variability enables more precise mapping of MASLD-related pathways and genes, but at the cost of not representing human inter-individual physiological diversity. Nevertheless, the choice of inbred mice is often necessary, especially when generating a colony of GEMs. Currently, several GEMs are available, including monogenetic, polygenetic, and liver-specific GEMs, with a well-established genetic background for metabolic studies and suitable for gene KO. Genetic alterations associated with fatty liver disease most commonly involve lipoprotein trafficking, glucose metabolism, adiposity/fat distribution, IR, or mitochondrial/endoplasmic reticulum biology.

Despite GEMs represent valuable tools for studying MASLD, each of them has advantages and limitations. Monogenic mouse models offer insights into the role of specific genes and usually replicate the key human metabolic alterations but may oversimplify the multifactorial nature of MASLD. Conversely, the strength of liver-specific genetic models lies in the study of specific molecular pathways without the confounding influence of systemic metabolic challenges. However, these mouse models can also exhibit unpredictable systemic alterations, potentially influencing the specific liver phenotype and lack of relevant interactions between the liver and adipose tissue, pancreas, and cardiovascular system. Moreover, these models may not be ideal for initial phenotyping of a novel gene's function, while whole-body KO may reveal complex metabolic and interorgan crosstalk that would be overlooked in a liver-specific model, offering broader insights into the gene's role in metabolic regulation. The choice of GEMs should therefore be carefully guided by the research question, balancing the goal of precise dissection of cell-specific mechanisms with the need to understand systemic complexity. Ideally, polygenetic mouse models for MASLD would help improve the translation of preclinical findings into human clinical applications but are currently underutilized because they are more expensive and time-consuming than using established models [56].

Recent insights into gene-environment interactions and health comorbidities have highlighted their significant role in MASLD susceptibility and severity in patients, with a particular focus on food composition in both humans and mice [38,57]. For this reason, GEMs are often also subjected to dietary variations, which complement the study of metabolic dysfunctions and molecular mechanisms—such as oxidative stress and ferroptosis—occurring at different stages of disease progression [32,40,56,58]. One of the main criticisms levelled at rodent diets is the lack of standardization that faithfully reflects human dietary patterns. Variability in macronutrient and micronutrient content may contribute to differing results among rodent studies and may hinder their translation into the clinical setting [59]. Despite this, one of the main dietary regimens used in MASLD models, often associated with GEMs, is WD.

Although the role of gene-environment interactions in the pathogenesis of MASLD has been widely recognized, an overlooked aspect is the sensitivity of different mouse models to husbandry conditions, depending on common practices and available laboratory resources. Interestingly, mouse housing temperature can impact liver disease modelling, and thermoneutrality (TN) conditions around 30 °C can exacerbate liver damage progression by influencing systemic metabolism through decreased thermogenesis and inflammation, compared to standard housing temperatures (20-24 °C) [31,32,55]. For instance, PWK/PhJ mice, fed WD and kept under TN conditions from 7 to 24 weeks of age, have been recently described as a promising mouse model with features of human MASH,

 doi:10.20944/preprints202602.1274.v1

showing more severe obesity and IR, higher liver enlargement and serum levels of cholesterol and transaminases compared to other mouse strains, including C57BL/6J [55]. Noteworthy, PWK/PhJ mice developed significant fibrosis and displayed distinct transcriptomic and mitochondrial alterations. Also, ten-week-old male C57BL/6J mice fed a similar WD for 13 weeks under TN showed more severe pathological, histological, and molecular features of MASLD than their counterparts raised at 22 °C [55].

In a comparative analysis of experimental conditions [60], it has been highlighted that TN could have an impact on the development of MASLD mainly in the early stages of the disease rather than in the more advanced ones; that diet composition plays a key role in shaping MASLD at thermal neutrality; and that TN rearing could reduce intragroup variability in response to WD feeding. Furthermore, it has been reported a complex crosstalk between liver and adipose tissue for the initiation and progression of MASLD depending on the housing temperature of the mice, including an altered hepatic response to white adipose tissue lipolysis and reduced brown adipose tissue activation in response to β3-adrenergic stimulation [60]. However, TN did not clearly affect MASH progression towards fibrosis in 8-week-old male C57BL/6J mice compared to those maintained at standard room temperature after 4 and 7 months of GAN, showing a comparable histological pattern of liver disease [61].

Taken together, these findings suggest that careful consideration of TN could help optimize mouse models of MASLD by significantly reducing the dietary intervention time, the number of animals required to model MASLD, and the interindividual variability. Despite this, its practical availability and management in laboratory animal facilities may vary [60].

A final important aspect is that most studies have been conducted in male mice, highlighting the need for future research on MASLD in females. Indeed, increasing evidence showed the protective role of estrogen in cardiovascular and metabolic diseases but in recent years it is also emerging MASLD health risks for women [32,62,63].

Within this complexity and the multitude of factors to be considered, ethical and practical aspects of each MASLD-related approach must also be taken into account. WD consumption for many weeks in wild type mice or GEMs increases experimental costs and may lead to various adverse health conditions (reduced food intake, weight loss, microbiota dysbiosis, chronic joint pain, neurobehavioral alterations) likely related to the progression of liver injury and IR [38]. A high-fructose diet negatively impacts osteogenesis and bone density in mouse models, predisposing to osteoporotic fractures [33]. Raising mice in TN is controversial because it affects the animals' metabolism and immune function, which can potentially alter experimental results depending on the research context [31,32]. Consequently, increased suffering and mortality not only pose significant animal welfare concerns but also operational challenges, such as the need to use more animals to maintain statistical power in later phases of the study.

The multifactorial nature of the disease and the difficulty in selecting an appropriate MASLD murine model contribute to the incomplete understanding of its pathogenic mechanisms, particularly those leading from simple steatosis to steatohepatitis. From this perspective, it is well established that excess dietary lipids and carbohydrates cause lipid droplet formation in hepatocytes, but these can be degraded to some extent by autophagy, preventing exceeding tissue storage and subsequent cellular dysfunction. Thus, the role of autophagy as an important regulator of lipid homeostasis has emerged, and its impairment may contribute to the accumulation of lipid droplets in liver tissue and the development of MASLD. For this reason, regulatory changes in hepatocyte autophagy due to overnutrition and the influence of this process in other organs, such as adipose tissue, are under investigation.

New Zealand Obese (NZO) mice, a polygenic model of metabolic syndrome and type2 diabetes, showed early obesity just at 22 weeks of age under standard diet (SD), similarly to older 39 weeks old C57BL/6J mice, and developed more pronounced MASLD when fed HFD (36% fat) for 16 weeks, findings overall related to decreased liver autophagy [64].

 doi:10.20944/preprints202602.1274.v1

Recently, a mouse model KO for mitogen-activated protein kinase 15 (MAPK15) on a C57BL/6J background has been characterized, highlighting a key role of this protein in the control of mammalian hepatic lipid homeostasis [65]. Specifically, wild-type and KO mice were fed a WD diet whose composition realistically mimicked the human imbalanced Western diet (38% fat, 0.2% cholesterol, 33% sucrose) from 8 to 24 weeks of age, and the phenotypic, metabolic, and imaging characteristics of MASLD were monitored in vivo from early to later experimental stages. Interestingly, KO male mice developed earlier and more severe MASLD outcomes, including diet-induced obesity, increased blood transaminases, cholesterol and glucose, and IR compared to their wild-type counterparts. Noteworthy, male KO mice developed early liver changes on ultrasound, indicative of progressive worsening of hepatic steatosis, and some in the SD group showed mild hepatic steatosis. Histological analysis confirmed the presence of more severe hepatic steatosis and mild inflammation and fibrosis in WD-fed male KO mice compared to controls, while, consistent with the literature, female KO mice showed a trend toward greater lipid accumulation in the liver compared to wild-type mice but showed a milder phenotype than males. Overall, we demonstrated that deletion of the MAPK15 gene, under WD stimulation, worsens the progression of MASLD in mice. Importantly, transcriptomic analysis highlighted increased MAPK15 expression in the liver of MASLD patients, suggesting a compensatory role in disease progression.

Beyond that, the role of adipose tissue-liver crosstalk in the pathogenesis of MASLD was specifically studied in young male C57BL/6J mice and in adipocyte-specific autophagy-related gene 7 (Atg7) KO mice fed a HFD (32% fat) for up to 8 months. Although no differences were evident between KO mice and controls under standard conditions, HFD promoted autophagy in adipose tissue only in wild-type mice, which showed worsening hepatic steatosis, inflammation and fibrosis [66]. Consequently, observations from this mouse model may suggest the potential of targeting autophagy in adipose tissue for MASLD/MASH treatment. However, these adipose-tissue specific KO mice display hypertrophy of subcutaneous fat, but atrophy of visceral fat, while humans with MASLD typically show augmented visceral adiposity, which is strongly associated with metabolic dysfunctions and increased cardiovascular risk. This discordant pattern, which rather mimics human lipodystrophy, further highlights the need to carefully select mouse models to study the pathophysiology of hepatic lipid accumulation in human MASLD, based on specific research questions.

Another key mechanism leading to hepatic steatosis occurs when fatty acid uptake and synthesis exceed the capacity of hepatocytes for lipid oxidation and export. Recently, the role of A-kinase anchoring protein 1 (AKAP1), a mitochondrial protein involved in energy balance, regulation of lipid homeostasis, and MASLD, has been studied in AKAP1-deficient mice, both systemically and specifically in hepatocytes. Intriguingly, AKAP1 KO diet-induced obesity mouse model on C57BL/6N background showed less severe weight gain and metabolic alterations, including hyperlipidemia and IR, as well as hepatic steatosis under HFD (60% fat) for 24 weeks, compared to wild type mice. Comparable results were reproduced in mice by treatment with AKAP1 inhibitors. Mechanistically, these findings were related to increased energy expenditure due to enhanced thermogenesis in brown fat via the activity of the mitochondrial enzyme acyl-CoA synthetase long-chain family member 1 (ACSL1). These findings were coherent with AKAP1 downregulation found in subcutaneous adipose tissues of obese patients, compared to lean controls [67].

To analyze AKAP1 activity in hepatocytes, without the interference of increased energy expenditure in adipose tissue on fat accumulation in the liver, the same research group developed tissue-specific AKAP1 KO mice on C57BL/6J background. Liver- specific KO mice showed worsening of hepatic steatosis and steatohepatitis under HFD (60% fat) or WD (40% fat, 0.2% cholesterol) combined with 45% glucose and 55% fructose in drinking water up to 24 weeks, while restoring hepatic AKAP1 by knocking down Glycerol-3-phosphate acyltransferase 1 (GPAT1) improved the disease [68]. Interestingly, in this mouse model, primarily the moderate-fat, moderate-cholesterol diet supplemented with complex sugars induced human-like histological features of MASH as early as 16 weeks, including hepatocyte ballooning and fibrosis associated with obesity, dyslipidemia, and

 doi:10.20944/preprints202602.1274.v1

IR. Mechanistically, AKAP1 can inhibit triglyceride synthesis in hepatocytes by phosphorylating and inactivating GPAT1, a mitochondrial outer membrane protein that converts acyl-CoAs to lysophosphatidic acid. This finding would be consistent with the clinical literature, which describes a loss-of-function GPAT1 genetic variant with a protective role against MASLD, while a gain-of-function mutation increases predisposition to the disease. Thus, this mouse model revealed that AKAP1 deficiency would predispose to hepatic steatosis mainly through positive regulation of triglyceride synthesis via enhanced mitochondrial GPAT activity, which appears as a novel potential therapeutic target.

Recently, young mice carrying the Ay (Agouti Yellow) mutation have been used to study MASLD. They were fed a diet high in fat (42%), cholesterol (0.2%), and sucrose (24%), and drinking water sweetened with fructose (23 g/L) and glucose (19 g/L) and developed hyperphagia, obesity, hypertriglyceridemia, IR and hepatic steatosis, including inflammation and fibrosis, as early as 16 weeks, progressing to more advanced lesions after 12 months [49]. Consequently, this model has been proposed to study MASLD pathophysiology and test new therapies. Indeed, 8-week-old male and female C57BL/6J mice fed a high-cholesterol WD (42% fat, 0.2% cholesterol) combined with fructose (23.1 g/l) and glucose (18.9 g/l) in the drinking for 25 weeks water up to 6 months of age, showed increased food intake, weight gain, liver-to-body weight ratio, steatosis and hepatocellular ballooning, but not inflammation and fibrosis, compared to controls [69]. Furthermore, relevant metabolic parameters, such as transaminases, blood glucose, insulin levels and total cholesterol, were significantly higher than in control mice. Consistent with previous literature, female mice showed less severe metabolic alterations and hepatic steatosis than males. Concordant metabolic and histological findings were highlighted in C57BL/6J mice of both sexes fed a high-cholesterol, high-sucrose diet (38% fat; 47% carbohydrate, 33% sucrose) with a comparable experimental design [70]. This model appears interesting because it resembles the human “fast food” diet, potentially helping to study of the human MASLD pathogenesis and preventive or therapeutic treatments [69].

Overall, these GEM studies could be useful to identify strategies for the prevention and treatment of obesity, with potential implications for MASLD research. On the other hand, MASLD, despite being generally associated with overweight or obesity, is increasingly being diagnosed in lean people as well, in relation to significant cardiovascular risk; so the presence of lean-MASLD necessitates the development of ad hoc animal models such as Lrpprc KO mice, which exhibit sex-dependent cardiometabolic impairments triggered by impaired mitochondrial integrity and β-oxidation [71].

Recently, also an important role of the intestinal compartment has been highlighted. Studies conducted in KO mice for Tm6sf2, a regulator of hepatic lipid metabolism expressed in liver and small intestine, have shown that intestinal Tm6sf2 deficiency primarily promotes MASH in both male and female mice, further worsening on CD or WD. Mechanistically, intestinal cells deficient in Tm6sf2 secrete more free fatty acids by interacting with fatty acid-binding protein 5, inducing intestinal barrier dysfunction, alterations in the microbiota and increases in lysophosphatidic acid, which is translocated to the liver, contributing to steatosis and inflammation [72].

Lately, polygenic models of obesity are emerging as new models of diet-induced MASLD. For instance, TALLYHO/JngJ and NONcNZO10/LtJ mouse strains, with a genetic predisposition to overweight while on a standard diet, were fed a HFD containing 1% of cholesterol and supplemented with fructose/sucrose (55/45%) in drinking water for 16 weeks [56]. Comparative pathology analysis showed that these mouse models developed good metabolic similarity and hepatocyte ballooning and steatosis, as well as mild inflammation and fibrosis comparable to the spectrum observed in the onset of human MASH. Furthermore, TALLYHO/JngJ mice developed signs of kidney damage similar to those of patients with cardiorenal syndrome. Interestingly, these models were useful in demonstrating the ability of empagliflozin, a sodium-glucose cotransporter 2 inhibitor, to significantly attenuate the histological outcomes of MASLD [56].

Since lipid-induced oxidative DNA damage in hepatocytes is strongly suspected to induce carcinogenesis, efforts are intensifying to develop mouse models that mimic the evolution of MASH

 doi:10.20944/preprints202602.1274.v1

and fibrosis into HCC, most frequently observed in GEM or specific strains of mice. Eight-week-old C57BL/6NJ mice, fed WD (42% kcal from fat, 0.2% cholesterol, 42.7% carbohydrate) and drinking water supplemented with 2% fructose and glucose for up to 54 weeks, developed hepatocellular ballooning, inflammation, and fibrosis as early as 16 weeks, with progressive worsening up to 32 weeks and beyond, as well as spontaneous HCC [47]. This substrain differs from the parental C57BL/6J by having a functional Nnt gene, and shows enhanced impairment of glucose metabolism, but similar susceptibility to metabolic diseases when on high-fat/high-sucrose diet [73].

A similar 36-week dietary intervention induced higher levels of transaminases and plasma cholesterol, as well as greater liver inflammation, fibrosis, and HCC incidence in adult Cyp2a12/Cyp2c70 knock-out (DKO) male mice compared to WT mice [74]. Considering interspecies differences, this DKO GEM lacks two enzymes responsible for increased bile acid hydrophilicity in mice, thus presenting a bile acid composition like that of humans. Therefore, evidence from this model suggests that accumulation of hydrophobic bile acids in the liver is a key mechanism promoting MASH/HCC progression and thus a potential preventive and therapeutic target.

Overall, these considerations underscore that careful selection of diet and its duration, mouse strain, study length, the use of GEM models, and careful attention to housing conditions is crucial when modeling MASLD. Although a wide and diverse array of models is currently available, they remain insufficient to fully unravel the complexities of MASLD. The development of polygenic models further aims to overcome the limitations of single-factor approaches, although predicting the complex interactions among genetic, dietary, and environmental factors—particularly when host-intrinsic factors such as microbiota contribute to variability—remains a significant challenge. Table 1 provides an attempt to summarize the main features of the most used models, intended to guide researchers in selecting the most appropriate approach.

Table 1. MASLD mouse models and their comparative pathological features relevant to translational research.

Mouse age and model	**Sex**	**MASLD induction**	**Key characteristics for MASLD research**		**Ref.**
			Liver	Systemic	
10-weeks-old C57BL/6J	Male	CD 20 weeks	Hepatomegaly Steatosis Inflammation Fibrosis HCC	↓ BW ↓ plasmatic transaminases, insulin and glucose	[35]
4-weeks-old C57BL/6J	Male	HFD 17 months	Hepatomegaly Steatosis	↑ BW ↑ IR Transcriptome changes in collagen and lipid regulatory genes	[38]
7 weeks-old NZO C57BL/6J	Male	HFD 32 weeks	Hepatomegaly Steatosis	↑ BW ↑ autophagy-related proteins	[64]
8-weeks-old C57BL/6J	Male and female	WD 17 weeks	Hepatomegaly Steatosis	↑ BW sexual dimorphism ↑ plasmatic transaminases, cholesterol, insulin and glucose In vivo heart, kidney, liver US alterations	[70]

 doi:10.20944/preprints202602.1274.v1

				Kidney alterations	
8-weeks-old C57BL/6J	Male	WD 16 weeks	Metabolic changes comparable to humans	Changes in lipidome and metabolome profiles comparable to those in humans	[42]
8-weeks-old C57BL/6N	Male	WD + fructose 10 weeks	Hepatomegaly Steatosis	↑ BW IR ↑ plasmatic transaminases, cholesterol, insulin and glucose autophagy-related transcriptome changes	[53]
6 weeks-old C57BL/6J	Male	WD + fructose/glucose 24 weeks	Hepatomegaly Steatosis Inflammation Fibrosis	↑ BW IR ↑ plasmatic transaminases, cholesterol, insulin and glucose ↑ lipogenic enzymes ↑ oxidative stress markers ↑ lipid peroxidation	[45]
8 weeks-old C57BL/6J	Male	WD + fructose/glucose 25 weeks	Hepatomegaly Steatosis	↑ BW IR ↑ plasmatic transaminases, cholesterol, insulin and glucose	[48]
10-weeks-old C57BL/6J	Male	WD + TN 13 weeks	Hepatomegaly Steatosis Inflammation Fibrosis	↑ BW IR ↑ plasmatic insulin and glucose Transcriptome changes in response to β3-adrenergic stimulation	[60]
8 weeks-old C57BL/6J	Male	GAN + TN 7 months	Steatosis Inflammation	↑ BW ↑ plasmatic transaminases	[61]

 doi:10.20944/preprints202602.1274.v1

8 weeks-old C57BL/6J	Male	GAN 44 weeks	Hepatomegaly Steatosis Inflammation Fibrosis	↑ BW IR ↑ plasmatic transaminases, cholesterol, insulin and glucose MASH-related transcriptomic alterations	[50]
6 weeks-old C57BL/6J	Male	GAN 10 weeks	Hepatomegaly Steatosis Mild inflammation	↑ BW ↑ plasmatic cholesterol Microbiota alterations	[46]
14 months-old C57BL/6J	Male and female	GAN 10 weeks	Hepatomegaly Accelerated steatosis and inflammation	↑ BW Sexual dimorphism Hepatomegaly ↑ plasmatic transaminases, cholesterol, insulin and glucose	[53]
6 weeks-old C57BL/6J	Male	GAN 72 weeks	Hepatomegaly Steatosis Inflammation Fibrosis HCC	↑ BW ↑ plasmatic transaminases ↑ fibrosis markers	[54]
8 weeks-old C57BL/6NJ	Male	WD + fructose/glucose 54 weeks	Hepatomegaly Steatosis Inflammation Fibrosis HCC	↑ BW ↑ plasmatic transaminases, cholesterol, insulin and glucose	[47]
7 weeks-old PWK/PhJ C57BL/6J	Male	WD + TN 18 weeks	Hepatomegaly Steatosis Inflammation Fibrosis	↑ BW IR ↑ plasmatic transaminases, cholesterol, insulin and glucose Transcriptomic and mitochondrial alterations	[55]
AKAP1 KO C57BL/6N	Male	HFD 24 weeks	Steatosis	↓ BW Hyperlipidemia ↑ thermogenesis	[67]

 doi:10.20944/preprints202602.1274.v1

8-weeks-old liver specific- AKAP1 KO C57BL/6J	Male	HFD/ WD + fructose/glucose 24 weeks	Hepatomegaly Steatosis Inflammation Fibrosis	↑ BW IR ↑ plasma lipids ↑ mitochondrial GPAT activity	[68]
8 weeks-old Atg7 KO C57BL/6	Male	HFD 8 months	Hepatomegaly Steatosis Inflammation Fibrosis	↓ BW ↑ plasmatic transaminases ↓ expression of autophagy-related proteins	[66]
8-weeks-old MAPK15 KO C57BL/6J	Male and female	WD 17 weeks	Hepatomegaly Steatosis Mild inflammation Fibrosis	↑ BW Sexual dimorphism ↑ plasmatic transaminases ↑ cholesterol ↑ insulin and glucose in vivo US alterations	[65]
8-weeks-old Ay C57BL/6J	Male	WD + fructose/glucose 12 months	Hepatomegaly Steatosis Inflammation Fibrosis	↑ BW IR ↑ plasma lipids	[49]
Liver specific-Lrpprc KO C57BL/6N	Male and female	SD 14 weeks	↓ Liver weight Steatosis Inflammation Fibrosis Mitochondrial disfunction ↑ ER stress markers	↓ BW Sexual dimorphism ↓ weight heart, adipose tissue, soleus ↓ insulin and glucose ↑ plasma lipids Cardiometabolic impairment	[71]
7 weeks-old intestine-specific Tm6sf2 KO C57BL/6	Male	CD/WD 8/14 weeks	Hepatomegaly Steatosis Mild inflammation	↑ BW ↑ plasmatic transaminases ↑ cholesterol Microbiota alterations	[72]
4 weeks-old TALLYHO/JngJ and NONcNZO10/LtJ	Female	HFD + fructose/glucose 16 weeks	Hepatomegaly Steatosis Inflammation Fibrosis Ballooning	↑ BW IR ↑ plasmatic transaminases ↑ cholesterol ↑ insulin and glucose Kidney injury	[56]

 doi:10.20944/preprints202602.1274.v1

11 weeks-old Cyp2a12/Cyp2c70 KO C57BL/6J	Male	WD + fructose/glucose 36 weeks	Hepatomegaly Steatosis Inflammation Fibrosis HCC	↑ BW ↑ plasmatic transaminases ↑ cholesterol ↑ insulin and glucose	[74]

Abbreviations: BW, body weight; CD, choline-deficient diet; ER, endoplasmic reticulum; GAN, Gubra Amylin diet; HCC, hepatocarcinoma; HFD, high fat diet; IR, insulin resistance; SD, standard diet; TN, thermoneutrality; WD, western diet.

In this perspective, also liver-humanized mice may be particularly valuable to study metabolism and effect of therapeutic molecules, because they closely replicate enzymatic features of human hepatocytes, while their use to study metabolic disorders is currently controversial [26].

3. Histopathological Findings in MASLD

From a histopathological perspective, MASLD in humans is characterized by a set of hallmark features, including steatosis—defined as fat accumulation in more than 5% of hepatocytes and often predominantly localized in zone 3—together with inflammation, hepatocellular ballooning, and variable degrees of fibrosis. As the disease progresses, MASLD may evolve into MASH, which is distinguished by more pronounced inflammation and ballooning and may ultimately progress to cirrhosis. Typical liver histological findings include lipid droplets, inflammatory infiltrates composed of macrophages, neutrophils, and lymphocytes, ballooned hepatocytes (enlarged and injured cells), Mallory–Denk bodies, and perivenular fibrosis [75–77], which can be exacerbated also by the activation of hepatic stellate cells (HSC) [78]. Indeed, HSC can transdifferentiate into fibrogenic myofibroblasts playing a critical role in the progression of MASLD into MASH and cirrhosis [78].

In murine models of MASLD, research efforts are therefore focused on recapitulating the key histopathological features observed in human disease. As reviewed by Vacca et al., [32], no single model currently reproduces all the phenotypic and histological characteristics of human MASLD. Some models effectively simulate the metabolic aspects of the disease but exhibit a milder histological phenotype, whereas others rapidly progress to MASH with significant fibrosis. Nevertheless, several key histologic features of MASLD can still be observed in the livers of these models. These include the presence of both microvesicular and macrovesicular steatosis with lipid droplets of varying sizes, hepatocellular ballooning (Figure 2), and, in more severe models, the development of fibrosis. In both human and murine studies, histological staining techniques such as hematoxylin and eosin (H&E), Masson's trichrome, and Oil Red O are commonly employed to visualize overall liver architecture, lipid accumulation, and the presence and extent of fibrosis, thereby enabling the systematic assessment and scoring of histopathological features according to the established scoring systems [76,79,80].

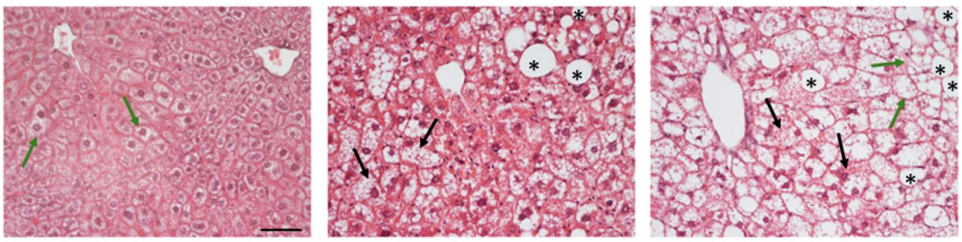

Figure 2. Representative H&E- stained images of murine liver sections illustrating different types of liver damage: macrovesicular steatosis (asterisks), microvesicular steatosis (green arrows), and hepatocellular ballooning (black arrows). Scale bar 50μm.

 doi:10.20944/preprints202602.1274.v1

The first histological scoring system in humans in the liver field was the METAVIR (initially used for hepatitis C and subsequently validated for almost all chronic liver diseases) which evaluates viral activity and classifies fibrosis into 4 states based on its extent [81]. Subsequently, in 2002, the National Institute of Diabetes, Kidney and Digestive Diseases validated the NAS (NAFLD Activity Score) histological scoring system [82] which provides a semiquantitative assessment of steatosis (0–3), lobular inflammation (0–3), hepatocellular ballooning (0–2), and fibrosis (0–4). There are also other scoring systems such as those by Brunt and Goodman, which differ slightly from NAS and incorporate the evaluation of portal inflammation, and more recently, the Fatty Liver Inhibition of Progression Pathology Consortium developed the SAF score algorithm (Steatosis, Activity and Fibrosis) which is able to distinguish between steatosis and necroinflammation [82–85]. Usually, basing on the NAS score, the pattern of liver injury, and the presence and severity of individual lesions, human biopsies can be classified as MASLD (not MASH), borderline MASH with a zone 1 pattern, borderline MASH with a zone 3 pattern, or definite MASH. Liang et al. [86] showed that NAS is also highly reproducible across rodent models and nowadays it remains widely used for evaluating MASLD in mice, although, from a histological perspective, mice exhibit different liver patterns compared to humans (Table 2).

Table 2. Histopathological differences between human and mice liver in MASLD.

Histological feature	Human MASLD/MASH	Murine MASLD/MASH models	Ref.
Steatosis	Diffuse macrovesicular steatosis, often centrilobular	Model dependent, sometimes prevalently microvesicular or patchy	[75–77,87]
Hepatocyte ballooning	Common in MASH	Often less pronounced than in humans	[56,75–77]
Lobular inflammation	Disseminated inflammatory infiltrates, mainly mononuclear cells	Inflammatory infiltrates milder; certain models show a predominance of intrahepatic T cells	[56,75–77]
Perisinusoidal / pericellular fibrosis	Progression to pericellular and periportal fibrosis in advanced MASH	Variable, some models display mild to moderate fibrosis with slow and less severe progression; others display rapid progression	[36,53,56,75–77]
Hepatic stellate cell (HSC) activation	HSC could have a role in exacerbating MASLD into MASH and inducing fibrosis	HSC activation occurs in response to injury, but with variable kinetics	[78,88–90]
Lobular zonation	Disease initially affects zone 3 and then spreads	Segmental or lobar heterogeneity	[42,75]

In mice, liver evaluation is typically performed after euthanasia, allowing collection of the entire organ and enabling accurate and comprehensive histological assessment and scoring. In human MASLD, biopsy is usually not recommended by guidelines, but it becomes necessary when non-invasive tests provide discordant data or when alternative aetiologies of liver disease are suspected. Indeed, it is precisely thanks to this technique that is possible to detect anatomical abnormalities and quantify the degree of liver inflammation associated with liver damage together with the evaluation of the extent of fibrosis [91]. In this context, the techniques most used in clinical practice are percutaneous and transvenous biopsies. The choice between these approaches is guided by individual patient characteristics, including the presence of ascites, BMI, coagulation disorders, thrombocythemia, and the need for concurrent hemodynamic evaluation or measurement of the hepatic venous pressure gradient. Percutaneous biopsy is performed in supine position and the localization of the liver between the sixth and ninth ribs is performed by percussion or with an

 doi:10.20944/preprints202602.1274.v1

ultrasound (US), Computed Tomography (CT) or Magnetic Resonance Imaging (MRI) guidance. In this case, it is essential to obtain a sample of intact liver tissue of an adequate size that allows observation of globular structures and portal tracts (at least 11 portal tracts obtainable using a 16-gauge needle) [92].

Given the bleeding risk associated with percutaneous biopsy, transvenous biopsy is recommended in patients with ascites or coagulopathy. The patient is sedated, and the procedure is performed under real-time fluoroscopic guidance and continuous cardiac monitoring to detect potential ventricular arrhythmias caused by catheter passage through the right atrium. In this case, the preferred approach is via the right internal jugular vein, which is catheterized under US guidance and local anaesthesia, with the patient in the supine position and the head rotated to expose the access site. From there, the guidewire reaches the inferior vena cava and advances to the right hepatic vein. A liver sample is obtained using an 18-19-gauge biopsy needle and must be at least 15 mm in diameter to be adequate for histological analysis.

Another commonly used approach is the transfemoral route, which offers the advantage of allowing measurement of the hepatic venous pressure gradient (HVPG), the gold standard for assessing portal hypertension. A significant increase in HVPG is indeed an important indicator of liver failure in patients with MASLD [93].

Another valid alternative is represented by laparoscopic biopsy, a technique that allows direct visualization of the liver parenchyma and immediate intervention with electrocauterization in the event of bleeding. Currently, biopsies can also be performed using mini laparoscopy, which employs optical systems and instruments smaller than 2 mm. These are introduced through a peri-umbilical incision and advanced to the liver parenchyma after the creation of a pneumoperitoneum [19].

One last important technique is endoscopic ultrasound–guided liver biopsy (EUS-LB), which is performed using an EUS echoendoscope capable of acquiring both ultrasound and doppler images for accurate visualization of vascular and anatomical structures. Tissue samples are typically obtained using a 19-gauge Tru-Cut needle, 19-gauge flexible fine-needle aspiration (FNA) needles, or fine-needle biopsy (FNB) needles. Compared with Tru-Cut and FNA needles, FNB needles allow the acquisition of liver tissue specimens that are more suitable for histological analysis [94].

All these biopsy techniques can lead to both major and minor complications, the most common of which include bleeding (intra-abdominal or intrahepatic bleeding occurs in approximately 10% of percutaneous or transvenous biopsies, although severe bleeding is reported in only about 2% of cases), pain (reported in 30–50% of patients), and infection. Mortality is estimated at less than 1 case per 1,000 procedures. Other potential complications include injury to adjacent organs and specific complications related to trans-jugular access, such as arrhythmias, neck hematoma, pneumothorax, transient Horner's syndrome, and arteriovenous fistula [92,95,96].

Considering these implications, in recent years, increasing efforts have been made to utilize data derived from liver biopsies to develop more innovative diagnostic approaches, including metabolomics-based methods and neural network–based models that integrate multiple histological features. In parallel, there is growing interest in the development of non-invasive diagnostic techniques (NITs), ranging from serological markers to various imaging techniques. These approaches may enable longitudinal monitoring and follow-up of the disease in a less burdensome manner for patients, while addressing key limitations of conventional histological scoring systems—such as the substantial time required for evaluation by experienced pathologists and the susceptibility to inter- and intra-observer variability [97–99]. For example, machine learning techniques are used to identify histological characteristics that may escape the human eye and can help predict disease progression and identify patients at risk of severe outcomes [100]. Besides, some Artificial Intelligence (AI) systems have been introduced: GENESIS and qFIBS use AI together with second harmonic fluorescence/two proton excitation techniques to quantify fibrosis, ballooning, steatosis, and inflammation in patients with MASH [101].

 doi:10.20944/preprints202602.1274.v1

In this context, focusing on the translational potential of imaging techniques from murine models to humans and the identification of shared biomarkers may be highly relevant for the development of future approaches to MASLD.

4. MASLD: Clinical and Experimental Imaging Assessment

The use of imaging is particularly recommended in humans, but it is also gaining traction in murine animal models. On one hand, scientific societies encourage the adoption of imaging techniques in humans to minimize invasiveness; on the other hand, monitoring animals with these techniques reduces inter-group variability and the number of animals required for research compared with conventional cross-sectional designs, which require sacrificing animals at each experimental time point. In both cases, imaging therefore represents a valuable tool for serially monitoring disease progression and/or treatment response. The World Federation for Ultrasound in Medicine and Biology (WFUMB) guidelines recommend liver biopsy and magnetic resonance imaging proton density fraction fat fraction (MRI-PDFF) as the gold standard methods for the diagnosis of MASLD. However, their limitations (e.g., invasiveness, relatively high costs, availability and patient compliance) have been overcome by newer, less invasive, and more accessible US-based software tools for hepatic fat quantification [102]. These advanced quantitative imaging techniques provide an objective measurement of liver fat content, which can be compared over time and correlates well with liver triglyceride content in a complementary manner to histological findings.

Among the wide range of imaging modalities, US Share Wave Elastography, MRI, and chemical shift–based water–fat separation techniques, such as magnetic resonance spectroscopy (MRS), have been employed [101]. In both species, these techniques enable non-invasive assessment of hepatic steatosis, liver morphology, and disease progression, supporting longitudinal and translational studies. The translational value of US and MRI between mice and humans depends heavily on intrinsic differences in anatomy, physiology, and technical requirements for imaging such small animals, as well as differences in perspective and resources. Despite the advantages, the translational gap in imaging studies between rodents and humans arises from the need for much higher imaging resolution in rodents, different clinical and experimental objectives, and logistical and ethical constraints. Nevertheless, better matching of clinical and preclinical imaging protocols may improve the translational potential of mouse models.

Conventional US is the first-line imaging technique for monitoring hepatic steatosis in humans and mice due to its safety and cost-effectiveness, although the accuracy of echogenicity and echotexture assessment in the liver parenchyma depends heavily on the sonographer's experience and the performance of the equipment. Nevertheless, quantitative US analysis of hepatic steatosis in humans has been shown to be more reproducible to screen MASLD [103], showing good sensitivity and specificity (about 90%) for the detection of moderate and severe hepatic steatosis but a more limited ability to detect mild and diffuse liver disease [104–106]. For this reason, there has been a shift from qualitative, semiquantitative B-mode imaging towards quantitative ultrasound (QUS) techniques that may provide more objective, reproducible, and accurate measurements of liver fat content, improving detection of mild steatosis. In mouse models the most technologically advanced US-based methods applied include US-induced thermal strain imaging, US molecular imaging using targeted microbubbles for disease markers and Shear Wave Elastography [107–109]. Previous efforts to characterize hepatic steatosis by texture analysis on ex vivo C57B6 and ob/ob mice US images, and recently on living C57BL/6J mice and MAPK15 KO mice, have demonstrated that complementary approaches, including semi-quantitative and parametric US data, are feasible and useful for the practical detection of longitudinal MASLD-related changes of the murine liver, with efficient processing times and good concordance with histology [20,110]. Recently, AI application to preclinical imaging have been stimulated to improve extraction of complex disease-related patterns also from US images [111].

 doi:10.20944/preprints202602.1274.v1

However, practical limitations such as proprietary software, sophisticated equipment, and specialized, time-consuming expertise limit the widespread availability of these techniques relative to other US quantitative techniques.

Other quantitative imaging techniques used for early diagnosis and disease monitoring in mouse models of hepatic steatosis include MRS, gradient-echo in-phase and out-of-phase imaging, and Dixon-based techniques. MRI can be used to accurately quantify fat in vivo in a whole-liver animal model of hepatic steatosis, showing good correlation with destructive techniques, such as histological analysis and liver lipid extraction. In parallel, in humans, a clinical study investigated the diagnostic performance of liver MRI-PDFF for fat quantification, showing good concordance with histopathology in obese patients undergoing bariatric surgery [112] and recently, a pilot study demonstrated the ability to assess changes in cell size and density as biomarkers of MASH by non-invasive MRI cytometry, with histology confirmation [113]. MRS also displayed good results both in human and mice. Indeed, newest MRS techniques allow for the non-invasive assessment of serial metabolic information in patients and preclinical models by directly measure the chemical composition of tissues based on the signals sent by protons; the proton produce a single peak in water and multiple peaks in fat due to different chemical bonds between protons and adjacent atoms [95]. Numerous studies have shown the validity of this test in humans where it detects hepatic steatosis [96,114] also in mild cases with a sensitivity of 80-91% and a specificity of 80-87% [115,116]. In parallel, MRS was used in vivo in CD-fed C57BL/6 male mice to longitudinally characterize changes in intrahepatic fatty acid and/or collagen composition from the early stage of MASLD to the more advanced stages of fibrosis-associated MASH, using a high resolution 9.4 T magnet and specialized sequences, such as stimulated echo acquisition mode (STEAM) combined with water suppression-variable pulse powers and optimized relaxation delays (VAPOR) algorithms or dynamic contrast enhanced (DCE) imaging using gadolinium-hydrazide, showing a good concordance with gas chromatography-mass spectrometry (GC–MS) and histology [117,118]. These studies highlighted that monitoring lipid or collagen composition, in addition to total fat, by implementing advanced MRI methods in mouse models of MASLD may provide new translational insights for non-invasive risk stratification in patients, considering the limitations of measuring liver fat content alone in the more advanced stages of so-called “burned” MASH where extensive fibrosis or cirrhosis has developed. In the same mouse model, preclinical high-field MRI was used to evaluate the efficacy of antifibrotic treatment with the polyethylene glycol fibroblast growth factor 21 (PEG-FGF21v) variant on liver steatosis and fibrosis, with clear correlations with histology, potentially guiding future translatable studies [119]. Similarly, HFD-fed C57BL/6J male mice treated with a glucagon-like peptide-1 receptor and glucagon receptor dual agonist, were monitored via 9.4 T scanner using proton density and R2* values to assess hepatic fat and iron content, respectively. Multiparametric MRI was able to highlight a more effective reduction of both imaging biomarkers compared to mice treated with a monoagonist, in correlation with histologic findings [120]. In particular, these findings shed new light on the potential value of regulating iron homeostasis as a therapeutic strategy for MASLD. Dixon- and STEAM-based, proton density MRS protocols were applied on 3T scanners to non-invasively characterize hepatic fatty acid changes in an HFD-fed eNOS KO mouse model, as well as for the assessment of treatment response to metformin. KO mice showed increased hepatic fat accumulation compared to control mice after 8 weeks of HFD, while metformin treatment significantly improved hepatic lipidomic profile compared to untreated mice [121]. Furthermore, in WD-fed female B6.Cg-Lepob/J mice, the combination of 1H-based liver fat fraction and 19F-based inflammation measurements using an 11.7 T small animal imaging scanner and Kupffer cells uptake of perfluorocarbon demonstrated the complementary utility of longitudinal quantification of multiple MRI biomarkers of disease to study MASLD liver pathology [122]. In line with current trends to non-invasively detect early stages of MASLD to improve treatment success, assessment of hepatic β-oxidation by [D15]-octanoate metabolism analysis and deuterium detection by MRI are emerging as translatable imaging modalities to study the clinical course of MASLD. Interestingly, HF-fed C57BL/6J mice were monitored by 11 T MRI after tail vein injection of [D15]octanoate for up to 36

 doi:10.20944/preprints202602.1274.v1

weeks, demonstrating that decreased β-oxidative efficiency in the steatotic liver could be a useful indicator of MASLD progression, occurring before overt structural changes such as hepatomegaly [123]. In summary, imaging may provide robust, non-invasive, and quantitative methods that are essential for the comprehensive and ethical study of hepatic steatosis progression and treatment in mouse models, but unfortunately, they allow a general comprehensive assessment of the liver but do not provide information on its microscopic characteristics, such as hepatocyte ballooning, lobular inflammation, Mallory bodies, and microvesicular and macrovesicular steatosis. Therefore, they cannot yet fully replace histological analysis of the liver obtained through sampling or biopsy, especially in animal models, where the assessment of histological features is a crucial step to understand how well the model reflects human disease. In this context a key strategy may be the use of complementary approaches that integrate imaging and histological analyses, in order to obtain the largest amount of information possible in a rapid and efficient manner.

5. Conclusion

Given the multifactorial and heterogeneous nature of MASLD in humans, no single animal model can adequately capture the full spectrum of disease manifestations. Instead, the rational selection of fit-for-purpose mouse models—guided by clinically relevant metabolic, histological, and non-invasive endpoints—is essential to address specific mechanistic and therapeutic questions. By focusing on the key characteristics that should guide the selection of appropriate animal models and by highlighting recent advances in non-invasive techniques applicable to both humans and mice, this review aims to help bridge the translational gap between human disease and preclinical research. The standardization of model selection and the harmonization of imaging protocols are expected to improve reproducibility, support the 3R principles, and enhance the predictive value of preclinical studies, ultimately accelerating the development of effective therapeutic strategies for MASLD.

Looking forward, future research in both humans and mice is expected to increasingly rely on stratified, phenotype-driven approaches that integrate histology, quantitative imaging and metabolic profiling. In clinical settings, this will enable more precise patient classification and the use of non-invasive tools to monitor disease progression and therapeutic response. In parallel, preclinical research is likely to expand the use of longitudinal imaging-based study designs, combined disease models (genetic+diet, diet+environmental factors) and humanized mouse models, including those incorporating human hepatocytes, immune components, or microbiota, to more faithfully recapitulate human-specific metabolic and inflammatory features of MASLD. Together, these advances will promote a more aligned, predictive, and personalized translational framework, ultimately improving the success of MASLD drug development and facilitating the implementation of multifactorial and combination-based therapeutic strategies.

Author Contributions: Conceptualization, D.B, S.G., L.L., M.G. V.B.; writing—original draft preparation, D.B, S.G., L.L., T.T, M.G. V.B.; writing—review and editing, D.B, S.G., L.L., T.T, M.G. L.G., L.F. G.I, M.C. V.B.; supervision, D.B, S.G., L.L., M.G., M.C., V.B. All authors have read and agreed to the published version of the manuscript.

Funding: This research received no external funding.

Institutional Review Board Statement: Not applicable.

Informed Consent Statement: Not applicable.

Data Availability Statement: No new data were created or analyzed in this study. Data sharing is not applicable to this article.

Conflicts of Interest: The authors declare no conflicts of interest.

Abbreviations

 doi:10.20944/preprints202602.1274.v1

The following abbreviations are used in this manuscript:

IR	Insulin Resistance
MASLD	Metabolic Dysfunction-Associated Steatotic Liver Disease
NAFLD	Non-Alcoholic Fatty Liver Disease
MASH	Metabolic Dysfunction-Associated Steatohepatitis
HCC	Hepatocellular carcinoma
BMI	Body Mass Index
PNPLA3	Patatin-like Phospholipase domain-containing 3
HSD17B13	17β-hydroxysteroid dehydrogenase-13
GCRK	Glucokinase regulatory protein gene
MBOAT7	Membrane-Bound O-Acyltransferase domain–containing 7
GLP-1	Glucagon-Like Peptide-1
PPAR	Peroxisome Proliferator–Activated Receptor
HFD	High Fat Diet
MCD	Methionine and/or Choline Deficient
WD	Western diet
GEM	Genetically Engineered Mouse
KO	Knock-Out
GAN	Gubra Amylin diet for non-alcoholic steatohepatitis
TN	Thermoneutrality
NZO	New Zealand Obese
SD	Standard Diet
MAPK15	Mitogen-Activated Protein Kinase 15
Atg7	Autophagy-related gene 7
AKAP1	A-Kinase Anchoring Protein 1
ACSL1	Acyl-CoA Synthetase Long-chain family member 1
GPAT1	Glycerol-3-Phosphate Acyltransferase 1
Ay	Agouti Yellow
DKO	Cyp2a12/Cyp2c70 knock-out
BW	Body Weight
ER	Endoplasmic Reticulum
HSC	Hepatic Stellate Cells
NAS	NAFLD Activity Score
H&E	Hematoxylin & Eosin
US	UltraSound
CT	Computed Tomography
MRI	Magnetic Resonance Imaging
HVPG	Hepatic Venous Pressure Gradient
EUS-LB	Endoscopic UltraSound-guided Liver Biopsy
FNA	Fine-Needle Aspiration
FNB	Fine-Needle Biopsy
NITs	Non-Invasive Tests
AI	Artificial Intelligence
WFUMB	World Federation for Ultrasound in Medicine and Biology
MRI-PDFF	Magnetic Resonance Imaging Proton Density Fat Fraction
MRS	Magnetic Resonance Spectroscopy
QUS	Quantitative UltraSound
STEAM	Stimulated Echo Acquisition Mode
DCE	Dynamic Contrast Enhanced
VAPOR	VAriable Power radiofrequency pulses with Optimized Relaxation delays
GC-MS	Gas Chromatography-Mass Spectrometry
PEG-FGF21v	Polyethylene glycol fibroblast growth factor 21 variant

References

1. Aron-Wisnewsky, J.; Vigliotti, C.; Witjes, J.; Le, P.; Holleboom, A.G.; Verheij, J.; Nieuwdorp, M.; Clément, K. Gut Microbiota and Human NAFLD: Disentangling Microbial Signatures from Metabolic Disorders. *Nat Rev Gastroenterol Hepatol* **2020**, *17*, 279–297, doi:10.1038/s41575-020-0269-9.

 doi:10.20944/preprints202602.1274.v1

2. Rinella, M.E.; Lazarus, J.V.; Ratziu, V.; Francque, S.M.; Sanyal, A.J.; Kanwal, F.; Romero, D.; Abdelmalek, M.F.; Anstee, Q.M.; Arab, J.P.; et al. A Multisociety Delphi Consensus Statement on New Fatty Liver Disease Nomenclature. *Hepatology* **2023**, *78*, 1966–1986, doi:10.1097/HEP.0000000000000520.
3. Stevanović-Silva, J.; Beleza, J.; Coxito, P.; Costa, R.C.; Ascensão, A.; Magalhães, J. Fit Mothers for a Healthy Future: Breaking the Intergenerational Cycle of Non-alcoholic Fatty Liver Disease with Maternal Exercise. *Eur J Clin Investigation* **2022**, *52*, e13596, doi:10.1111/eci.13596.
4. Maliken, B.D.; Nelson, J.E.; Klintworth, H.M.; Beauchamp, M.; Yeh, M.M.; Kowdley, K.V. Hepatic Reticuloendothelial System Cell Iron Deposition Is Associated with Increased Apoptosis in Nonalcoholic Fatty Liver Disease. *Hepatology* **2013**, *57*, 1806–1813, doi:10.1002/hep.26238.
5. Younossi, Z.M.; Golabi, P.; Paik, J.M.; Henry, A.; Van Dongen, C.; Henry, L. The Global Epidemiology of Nonalcoholic Fatty Liver Disease (NAFLD) and Nonalcoholic Steatohepatitis (NASH): A Systematic Review. *Hepatology* **2023**, *77*, 1335–1347, doi:10.1097/HEP.0000000000000004.
6. Huo, Z.; Chen, Y.; Huang, Y.; Yang, Z.; Long, Y.; Zhang, Q.; Chen, S.; Wang, G.; Zhu, S.; Sun, D.; et al. Long-Term Prognosis of Lean MASLD: Evidence from Three Population-Based Prospective Cohorts. *Gut* **2025**, gutjnl-2025-336127, doi:10.1136/gutjnl-2025-336127.
7. Ha, S.; Wong, V.W.-S.; Zhang, X.; Yu, J. Interplay between Gut Microbiome, Host Genetic and Epigenetic Modifications in MASLD and MASLD-Related Hepatocellular Carcinoma. *Gut* **2024**, *74*, 141–152, doi:10.1136/gutjnl-2024-332398.
8. Jegodzinski, L.; Rudolph, L.; Castven, D.; Sayk, F.; Rout, A.K.; Föh, B.; Hölzen, L.; Meyhöfer, S.; Schenk, A.; Weber, S.N.; et al. PNPLA3 I148M Variant Links to Adverse Metabolic Traits in MASLD during Fasting and Feeding. *JHEP Rep* **2025**, *7*, 101450, doi:10.1016/j.jhepr.2025.101450.
9. Su, W.; Wang, Y.; Jia, X.; Wu, W.; Li, L.; Tian, X.; Li, S.; Wang, C.; Xu, H.; Cao, J.; et al. Comparative Proteomic Study Reveals 17β-HSD13 as a Pathogenic Protein in Nonalcoholic Fatty Liver Disease. *Proc Natl Acad Sci U S A* **2014**, *111*, 11437–11442, doi:10.1073/pnas.1410741111.
10. Orho-Melander, M.; Melander, O.; Guiducci, C.; Perez-Martinez, P.; Corella, D.; Roos, C.; Tewhey, R.; Rieder, M.J.; Hall, J.; Abecasis, G.; et al. Common Missense Variant in the Glucokinase Regulatory Protein Gene Is Associated With Increased Plasma Triglyceride and C-Reactive Protein but Lower Fasting Glucose Concentrations. *Diabetes* **2008**, *57*, 3112–3121, doi:10.2337/db08-0516.
11. Chandrasekaran, P.; Weiskirchen, R. The Pivotal Role of the Membrane-Bound O-Acyltransferase Domain Containing 7 in Non-Alcoholic Fatty Liver Disease. *Livers* **2023**, *4*, 1–14, doi:10.3390/livers4010001.
12. O'Hare, E.A.; Yang, R.; Yerges-Armstrong, L.M.; Sreenivasan, U.; McFarland, R.; Leitch, C.C.; Wilson, M.H.; Narina, S.; Gorden, A.; Ryan, K.A.; et al. TM6SF2 Rs58542926 Impacts Lipid Processing in Liver and Small Intestine. *Hepatology* **2017**, *65*, 1526–1542, doi:10.1002/hep.29021.
13. Nemer, M.; Osman, F.; Said, A. Dietary Macro and Micronutrients Associated with MASLD: Analysis of a National US Cohort Database. *Annals of Hepatology* **2024**, *29*, 101491, doi:10.1016/j.aohep.2024.101491.
14. Hong, F.; Radaeva, S.; Pan, H.; Tian, Z.; Veech, R.; Gao, B. Interleukin 6 Alleviates Hepatic Steatosis and Ischemia/Reperfusion Injury in Mice with Fatty Liver Disease. *Hepatology* **2004**, *40*, 933–941, doi:10.1002/hep.20400.
15. Zheng, Y.; Huang, C.; Zhao, L.; Chen, Y.; Liu, F. Regulation of Decorin by Ursolic Acid Protects against Non-Alcoholic Steatohepatitis. *Biomedicine & Pharmacotherapy* **2021**, *143*, 112166, doi:10.1016/j.biopha.2021.112166.
16. Shen, F.; Zheng, R.-D.; Sun, X.-Q.; Ding, W.-J.; Wang, X.-Y.; Fan, J.-G. Gut Microbiota Dysbiosis in Patients with Non-Alcoholic Fatty Liver Disease. *Hepatobiliary & Pancreatic Diseases International* **2017**, *16*, 375–381, doi:10.1016/S1499-3872(17)60019-5.
17. Drygalski, K. Pharmacological Treatment of MASLD: Contemporary Treatment and Future Perspectives. *IJMS* **2025**, *26*, 6518, doi:10.3390/ijms26136518.
18. Hudson, D.; Afzaal, T.; Bualbanat, H.; AlRamdan, R.; Howarth, N.; Parthasarathy, P.; AlDarwish, A.; Stephenson, E.; Almahanna, Y.; Hussain, M.; et al. Modernizing Metabolic Dysfunction-Associated Steatotic Liver Disease Diagnostics: The Progressive Shift from Liver Biopsy to Noninvasive Techniques. *Therap Adv Gastroenterol* **2024**, *17*, 17562848241276334, doi:10.1177/17562848241276334.

 doi:10.20944/preprints202602.1274.v1

19. Tacke, F.; Horn, P.; Wai-Sun Wong, V.; Ratziu, V.; Bugianesi, E.; Francque, S.; Zelber-Sagi, S.; Valenti, L.; Roden, M.; Schick, F.; et al. EASL–EASD–EASO Clinical Practice Guidelines on the Management of Metabolic Dysfunction-Associated Steatotic Liver Disease (MASLD). *Journal of Hepatology* **2024**, *81*, 492–542, doi:10.1016/j.jhep.2024.04.031.
20. Gargiulo, S.; Gramanzini, M.; Bonente, D.; Tamborrino, T.; Inzalaco, G.; Gherardini, L.; Franci, L.; Bertelli, E.; Barone, V.; Chiariello, M. Preclinical Application of Computer-Aided High-Frequency Ultrasound (HFUS) Imaging: A Preliminary Report on the In Vivo Characterization of Hepatic Steatosis Progression in Mouse Models. *J. Imaging* **2025**, *11*, 369, doi:10.3390/jimaging11100369.
21. Pelechá, M.; Villanueva-Bádenas, E.; Timor-López, E.; Donato, M.T.; Tolosa, L. Cell Models and Omics Techniques for the Study of Nonalcoholic Fatty Liver Disease: Focusing on Stem Cell-Derived Cell Models. *Antioxidants* **2021**, *11*, 86, doi:10.3390/antiox11010086.
22. Caddeo, A.; Maurotti, S.; Kovooru, L.; Romeo, S. 3D Culture Models to Study Pathophysiology of Steatotic Liver Disease. *Atherosclerosis* **2024**, *393*, 117544, doi:10.1016/j.atherosclerosis.2024.117544.
23. Youhanna, S.; Taebnia, N.; Liang, Y.; Cheng, N.; Wang, Y.; Michel, M.; Lauschke, V.M. Primary Human Tissue Models for Metabolic Dysfunction-Associated Liver Disease - toward Streamlining Drug Discovery with Patient-Derived Assays. *Advanced Biology* **2025**, *9*, e00337, doi:10.1002/adbi.202500337.
24. Kwon, Y.; Gottmann, P.; Wang, S.; Tissink, J.; Motzler, K.; Sekar, R.; Albrecht, W.; Cadenas, C.; Hengstler, J.G.; Schürmann, A.; et al. Induction of Steatosis in Primary Human Hepatocytes Recapitulates Key Pathophysiological Aspects of Metabolic Dysfunction-Associated Steatotic Liver Disease. *Journal of Hepatology* **2025**, *82*, 18–27, doi:10.1016/j.jhep.2024.06.040.
25. Kruepunga, N.; Hakvoort, T.B.M.; Hikspoors, J.P.J.M.; Köhler, S.E.; Lamers, W.H. Anatomy of Rodent and Human Livers: What Are the Differences? *Biochimica et Biophysica Acta (BBA) - Molecular Basis of Disease* **2019**, *1865*, 869–878, doi:10.1016/j.bbadis.2018.05.019.
26. Luo, Y.; Lu, H.; Peng, D.; Ruan, X.; Eugene Chen, Y.; Guo, Y. Liver-humanized Mice: A Translational Strategy to Study Metabolic Disorders. *Journal Cellular Physiology* **2022**, *237*, 489–506, doi:10.1002/jcp.30610.
27. Nagarajan, P. Genetically Modified Mouse Models for the Study of Nonalcoholic Fatty Liver Disease. *WJG* **2012**, *18*, 1141, doi:10.3748/wjg.v18.i11.1141.
28. Jahn, D.; Kircher, S.; Hermanns, H.M.; Geier, A. Animal Models of NAFLD from a Hepatologist's Point of View. *Biochimica et Biophysica Acta (BBA) - Molecular Basis of Disease* **2019**, *1865*, 943–953, doi:10.1016/j.bbadis.2018.06.023.
29. Flessa, C.-M.; Nasiri-Ansari, N.; Kyrou, I.; Leca, B.M.; Lianou, M.; Chatzigeorgiou, A.; Kaltsas, G.; Kassi, E.; Randeva, H.S. Genetic and Diet-Induced Animal Models for Non-Alcoholic Fatty Liver Disease (NAFLD) Research. *IJMS* **2022**, *23*, 15791, doi:10.3390/ijms232415791.
30. Fu, Y.; Hua, Y.; Alam, N.; Liu, E. Progress in the Study of Animal Models of Metabolic Dysfunction-Associated Steatotic Liver Disease. *Nutrients* **2024**, *16*, 3120, doi:10.3390/nu16183120.
31. Cui, X.; Li, H.; Li, L.; Xie, C.; Gao, J.; Chen, Y.; Zhang, H.; Hao, W.; Fu, J.; Guo, H. Rodent Model of Metabolic Dysfunction-associated Fatty Liver Disease: A Systematic Review. *J of Gastro and Hepatol* **2025**, *40*, 48–66, doi:10.1111/jgh.16749.
32. Vacca, M.; Kamzolas, I.; Harder, L.M.; Oakley, F.; Trautwein, C.; Hatting, M.; Ross, T.; Bernardo, B.; Oldenburger, A.; Hjuler, S.T.; et al. An Unbiased Ranking of Murine Dietary Models Based on Their Proximity to Human Metabolic Dysfunction-Associated Steatotic Liver Disease (MASLD). *Nat Metab* **2024**, *6*, 1178–1196, doi:10.1038/s42255-024-01043-6.
33. Chen, J.; Jiang, X. A High-Fructose Diet Leads to Osteoporosis by Suppressing the Expression of Thrb and Facilitating the Accumulation of Cholesterol. *Cell Death Discov.* **2025**, *11*, 159, doi:10.1038/s41420-025-02445-5.
34. Estévez-Vázquez, O.; Benedé-Ubieto, R.; Guo, F.; Gómez-Santos, B.; Aspichueta, P.; Reissing, J.; Bruns, T.; Sanz-García, C.; Sydor, S.; Bechmann, L.P.; et al. Fat: Quality, or Quantity? What Matters Most for the Progression of Metabolic Associated Fatty Liver Disease (MAFLD). *Biomedicines* **2021**, *9*, 1289, doi:10.3390/biomedicines9101289.
35. Nielsen, M.H.; Nøhr-Meldgaard, J.; Møllerhøj, M.B.; Oró, D.; Pors, S.E.; Andersen, M.W.; Kamzolas, I.; Petsalaki, E.; Vacca, M.; Harder, L.M.; et al. Characterization of Six Clinical Drugs and Dietary Intervention

 doi:10.20944/preprints202602.1274.v1

in the Nonobese CDAA-HFD Mouse Model of MASH and Progressive Fibrosis. *American Journal of Physiology-Gastrointestinal and Liver Physiology* **2025**, *328*, G51–G71, doi:10.1152/ajpgi.00110.2024.

36. Li, H.; Toth, E.; Cherrington, N.J. Asking the Right Questions With Animal Models: Methionine- and Choline-Deficient Model in Predicting Adverse Drug Reactions in Human NASH. *Toxicological Sciences* **2018**, *161*, 23–33, doi:10.1093/toxsci/kfx253.
37. Fang, T.; Wang, H.; Pan, X.; Little, P.J.; Xu, S.; Weng, J. Mouse Models of Nonalcoholic Fatty Liver Disease (NAFLD): Pathomechanisms and Pharmacotherapies. *Int. J. Biol. Sci.* **2022**, *18*, 5681–5697, doi:10.7150/ijbs.65044.
38. Pompili, S.; Vetuschi, A.; Gaudio, E.; Tessitore, A.; Capelli, R.; Alesse, E.; Latella, G.; Sferra, R.; Onori, P. Long-Term Abuse of a High-Carbohydrate Diet Is as Harmful as a High-Fat Diet for Development and Progression of Liver Injury in a Mouse Model of NAFLD/NASH. *Nutrition* **2020**, *75–76*, 110782, doi:10.1016/j.nut.2020.110782.
39. Maddie, N.; Chacko, N.; Matatov, D.; Carrillo-Sepulveda, M.A. Western Diet Promotes the Progression of Metabolic Dysfunction-associated Steatotic Liver Disease in Association with Ferroptosis in Male Mice. *Physiological Reports* **2024**, *12*, e70139, doi:10.14814/phy2.70139.
40. Meijnikman, A.S.; Fondevila, M.F.; Arrese, M.; Kisseleva, T.; Bataller, R.; Schnabl, B. Towards More Consistent Models and Consensual Terminology in Preclinical Research for Steatotic Liver Disease. *Journal of Hepatology* **2025**, *82*, 760–766, doi:10.1016/j.jhep.2024.11.025.
41. Svobodová, G.; Horní, M.; Velecká, E.; Boušová, I. Metabolic Dysfunction-Associated Steatotic Liver Disease-Induced Changes in the Antioxidant System: A Review. *Arch Toxicol* **2025**, *99*, 1–22, doi:10.1007/s00204-024-03889-x.
42. Ma, X.; Bian, W.; Song, W.; Lu, Y.; Wang, Z.; Yao, Z.; Xuan, Q. Metabolome Profiling across Liver Lobes and Metabolic Shifts of the MASLD Mice. *Genes Nutr* **2025**, *20*, 9, doi:10.1186/s12263-025-00768-7.
43. Li, Y.-Q.; Huang, C.; Chen, J.; Yang, S.; Cheng, J.; Chen, H.; Zhou, Y. Identification of the Role of Sugar-Sweetened Beverages in the Progression of a Murine Metabolic Dysfunction-Associated Steatotic Liver Disease Model. *Front. Nutr.* **2025**, *12*, 1710267, doi:10.3389/fnut.2025.1710267.
44. Jeon, H.J.; Rou, W.S.; Kim, S.H.; Lee, B.S.; Kim, H.N.; Choi, H.-G.; Seo, J.; Eun, H.S.; Jung, S. Sugar-Sweetened Beverage Consumption and Metabolic Dysfunction-Associated Steatotic Liver Disease: A Beverage Type-Specific Analysis Using Korea National Health and Nutrition Examination Survey. *Epidemiol Health* **2025**, *47*, e2025038, doi:10.4178/epih.e2025038.
45. Hsu, W.-F.; Lee, M.-H.; Lii, C.-K.; Peng, C.-Y. No Difference in Liver Damage Induced by Isocaloric Fructose or Glucose in Mice with a High-Fat Diet. *Nutrients* **2024**, *16*, 3571, doi:10.3390/nu16203571.
46. Zhang, Z.; Qin, X.; Yi, T.; Li, Y.; Li, C.; Zeng, M.; Luo, H.; Lin, X.; Xie, J.; Xia, B.; et al. Gubra Amylin-NASH Diet Induced Nonalcoholic Fatty Liver Disease Associated with Histological Damage, Oxidative Stress, Immune Disorders, Gut Microbiota, and Its Metabolic Dysbiosis in Colon. *Molecular Nutrition Food Res* **2024**, *68*, 2300845, doi:10.1002/mnfr.202300845.
47. Green, C.D.; Weigel, C.; Brown, R.D.R.; Bedossa, P.; Dozmorov, M.; Sanyal, A.J.; Spiegel, S. A New Preclinical Model of Western Diet-induced Progression of Non-alcoholic Steatohepatitis to Hepatocellular Carcinoma. *The FASEB Journal* **2022**, *36*, e22372, doi:10.1096/fj.202200346R.
48. Makri, E.S.; Xanthopoulos, K.; Mavrommatis Parasidis, P.; Makri, E.; Pettas, S.; Tsingotjidou, A.; Cheva, A.; Ballaouri, I.; Gerou, S.; Goulas, A.; et al. Partial Validation of a Six-Month High-Fat Diet and Fructose-Glucose Drink Combination as a Mouse Model of Nonalcoholic Fatty Liver Disease. *Endocrine* **2024**, *85*, 704–716, doi:10.1007/s12020-024-03769-5.
49. Khoj, D.; Huang, R.; Altvater, E.; Ishfaq, Z.N.; Jiang, X.; Axen, K.V.; Caviglia, J.M. Mouse Model of Metabolic Dysfunction-Associated Steatotic Liver Disease with Fibrosis. *JoVE* **2025**, 68294, doi:10.3791/68294.
50. Hansen, H.H.; Ægidius, H.M.; Oró, D.; Evers, S.S.; Heebøll, S.; Eriksen, P.L.; Thomsen, K.L.; Bengtsson, A.; Veidal, S.S.; Feigh, M.; et al. Human Translatability of the GAN Diet-Induced Obese Mouse Model of Non-Alcoholic Steatohepatitis. *BMC Gastroenterol* **2020**, *20*, 210, doi:10.1186/s12876-020-01356-2.
51. Dutta, S.; Sengupta, P. Men and Mice: Relating Their Ages. *Life Sciences* **2016**, *152*, 244–248, doi:10.1016/j.lfs.2015.10.025.

 doi:10.20944/preprints202602.1274.v1

52. Jackson, S.J.; Andrews, N.; Ball, D.; Bellantuono, I.; Gray, J.; Hachoumi, L.; Holmes, A.; Latcham, J.; Petrie, A.; Potter, P.; et al. Does Age Matter? The Impact of Rodent Age on Study Outcomes. *Lab Anim* **2017**, *51*, 160–169, doi:10.1177/0023677216653984.
53. Li, X.; Lu, Y.; Liang, X.; Zhou, X.; Li, D.; Zhang, Z.; Niu, Y.; Liu, S.; Ye, L.; Zhang, R. A New NASH Model in Aged Mice with Rapid Progression of Steatohepatitis and Fibrosis. *PLoS ONE* **2023**, *18*, e0286257, doi:10.1371/journal.pone.0286257.
54. Hansen, H.H.; Pors, S.; Andersen, M.W.; Vyberg, M.; Nøhr-Meldgaard, J.; Nielsen, M.H.; Oró, D.; Madsen, M.R.; Lewinska, M.; Møllerhøj, M.B.; et al. Semaglutide Reduces Tumor Burden in the GAN Diet-Induced Obese and Biopsy-Confirmed Mouse Model of NASH-HCC with Advanced Fibrosis. *Sci Rep* **2023**, *13*, 23056, doi:10.1038/s41598-023-50328-5.
55. Benegiamo, G.; Von Alvensleben, G.V.G.; Rodríguez-López, S.; Goeminne, L.J.E.; Bachmann, A.M.; Morel, J.-D.; Broeckx, E.; Ma, J.Y.; Carreira, V.; Youssef, S.A.; et al. The Genetic Background Shapes the Susceptibility to Mitochondrial Dysfunction and NASH Progression. *Journal of Experimental Medicine* **2023**, *220*, e20221738, doi:10.1084/jem.20221738.
56. Hupa-Breier, K.L.; Schenk, H.; Campos-Murguia, A.; Wellhöner, F.; Heidrich, B.; Dywicki, J.; Hartleben, B.; Böker, C.; Mall, J.; Terkamp, C.; et al. Novel Translational Mouse Models of Metabolic Dysfunction-Associated Steatotic Liver Disease Comparable to Human MASLD with Severe Obesity. *Molecular Metabolism* **2025**, *93*, 102104, doi:10.1016/j.molmet.2025.102104.
57. Lee, Y.-C.; Lee, H.S.; Jeon, S.; Lee, Y.-J.; Kwon, Y.-J.; Lee, J.-W. Assessing Nutritional Factors for Metabolic Dysfunction-Associated Steatotic Liver Disease via Diverse Statistical Tools. *Diabetes Metab J* **2026**, *50*, 178–189, doi:10.4093/dmj.2025.0026.
58. Mann, J.P.; Semple, R.K.; Armstrong, M.J. How Useful Are Monogenic Rodent Models for the Study of Human Non-Alcoholic Fatty Liver Disease? *Front. Endocrinol.* **2016**, *7*, doi:10.3389/fendo.2016.00145.
59. Hintze, K.J.; Benninghoff, A.D.; Cho, C.E.; Ward, R.E. Modeling the Western Diet for Preclinical Investigations. *Advances in Nutrition* **2018**, *9*, 263–271, doi:10.1093/advances/nmy002.
60. Martin, C.M.P.; Polizzi, A.; Alquier-Bacquié, V.; Huillet, M.; Rives, C.; Dauriat, C.J.G.; Bruse, J.; Melin, V.; Naylies, C.; Lippi, Y.; et al. Thermoneutral Housing Worsens MASLD and Reveals Defective Brown Adipose Tissue Response to B3-Adrenergic Stimulation. *iScience* **2025**, *28*, 113221, doi:10.1016/j.isci.2025.113221.
61. Blok, N.B.; Myronovych, A.; McMahon, G.; Bozadjieva-Kramer, N.; Seeley, R.J. The Evolution of Steatosis and Fibrosis in Mice on a MASH-Inducing Diet and the Effects of Housing Temperature. *American Journal of Physiology-Endocrinology and Metabolism* **2025**, *328*, E513–E523, doi:10.1152/ajpendo.00401.2024.
62. Jancova, P.; Ismail, K.; Vistejnova, L. Relationship between MASLD and Women's Health: A Review. *Womens Health (Lond Engl)* **2025**, *21*, 17455057251376883, doi:10.1177/17455057251376883.
63. Alves, E.S.; Santos, J.D.M.; Cruz, A.G.; Camargo, F.N.; Talarico, C.H.Z.; Santos, A.R.M.; Silva, C.A.A.; Morgan, H.J.N.; Matos, S.L.; Araujo, L.C.C.; et al. Hepatic Estrogen Receptor Alpha Overexpression Protects Against Hepatic Insulin Resistance and MASLD. *Pathophysiology* **2025**, *32*, 1, doi:10.3390/pathophysiology32010001.
64. Korovila, I.; Höhn, A.; Jung, T.; Grune, T.; Ott, C. Reduced Liver Autophagy in High-Fat Diet Induced Liver Steatosis in New Zealand Obese Mice. *Antioxidants* **2021**, *10*, 501, doi:10.3390/antiox10040501.
65. Inzalaco, G.; Gargiulo, S.; Bonente, D.; Gherardini, L.; Franci, L.; Lorito, N.; Del Turco, S.; Tatoni, D.; Tamborrino, T.; Galvagni, F.; et al. MAPK15 Controls Intracellular Lipid Uptake and Protects Mammalian Liver from Steatotic Disease. *Hepatology Communications* **2026**, *10*, doi:10.1097/HC9.0000000000000870.
66. Sakane, S.; Hikita, H.; Shirai, K.; Myojin, Y.; Sasaki, Y.; Kudo, S.; Fukumoto, K.; Mizutani, N.; Tahata, Y.; Makino, Y.; et al. White Adipose Tissue Autophagy and Adipose-Liver Crosstalk Exacerbate Nonalcoholic Fatty Liver Disease in Mice. *Cellular and Molecular Gastroenterology and Hepatology* **2021**, *12*, 1683–1699, doi:10.1016/j.jcmgh.2021.07.008.
67. Ji, L.; Zhao, Y.; He, L.; Zhao, J.; Gao, T.; Liu, F.; Qi, B.; Kang, F.; Wang, G.; Zhao, Y.; et al. *X1AKAP1* Deficiency Attenuates Diet-Induced Obesity and Insulin Resistance by Promoting Fatty Acid Oxidation and Thermogenesis in Brown Adipocytes. *Advanced Science* **2022**, *9*, 2204669, doi:10.1002/advs.202204669.

 doi:10.20944/preprints202602.1274.v1

68. He, L.; She, X.; Guo, L.; Gao, M.; Wang, S.; Lu, Z.; Guo, H.; Li, R.; Nie, Y.; Xing, J.; et al. Hepatic AKAP1 Deficiency Exacerbates Diet-Induced MASLD by Enhancing GPAT1-Mediated Lysophosphatidic Acid Synthesis. *Nat Commun* **2025**, *16*, 4286, doi:10.1038/s41467-025-58790-7.
69. Makri, E.S.; Mouskeftara, T.; Gika, H.; Xanthopoulos, K.; Makri, E.; Mavrommatis-Parasidis, P.; Tsingotjidou, A.; Cheva, A.; Goulas, A.; Polyzos, S.A. Serum and Liver Lipidome Following Empagliflozin Administration for Six Months in a Fast Food Diet Mouse Model. *IJMS* **2025**, *26*, 9273, doi:10.3390/ijms26199273.
70. Gargiulo, S.; Barone, V.; Bonente, D.; Tamborrino, T.; Inzalaco, G.; Gherardini, L.; Bertelli, E.; Chiariello, M. Integrated Ultrasound Characterization of the Diet-Induced Obesity (DIO) Model in Young Adult C57bl/6j Mice: Assessment of Cardiovascular, Renal and Hepatic Changes. *J. Imaging* **2024**, *10*, 217, doi:10.3390/jimaging10090217.
71. Burelle, C.; Clapatiuc, V.; Deschênes, S.; Cuillerier, A.; De Loof, M.; Higgins, M.-È.; Boël, H.; Daneault, C.; Chouinard, B.; Clavet, M.-É.; et al. A Genetic Mouse Model of Lean-NAFLD Unveils Sexual Dimorphism in the Liver-Heart Axis. *Commun Biol* **2024**, *7*, 356, doi:10.1038/s42003-024-06035-6.
72. Zhang, X.; Lau, H.C.-H.; Ha, S.; Liu, C.; Liang, C.; Lee, H.W.; Ng, Q.W.-Y.; Zhao, Y.; Ji, F.; Zhou, Y.; et al. Intestinal TM6SF2 Protects against Metabolic Dysfunction-Associated Steatohepatitis through the Gut–Liver Axis. *Nat Metab* **2025**, *7*, 102–119, doi:10.1038/s42255-024-01177-7.
73. Fisher-Wellman, K.H.; Ryan, T.E.; Smith, C.D.; Gilliam, L.A.A.; Lin, C.-T.; Reese, L.R.; Torres, M.J.; Neufer, P.D. A Direct Comparison of Metabolic Responses to High-Fat Diet in C57BL/6J and C57BL/6NJ Mice. *Diabetes* **2016**, *65*, 3249–3261, doi:10.2337/db16-0291.
74. Ueda, H.; Honda, A.; Miyazaki, T.; Morishita, Y.; Hirayama, T.; Iwamoto, J.; Ikegami, T. High-Fat/High-Sucrose Diet Results in a High Rate of MASH with HCC in a Mouse Model of Human-like Bile Acid Composition. *Hepatology Communications* **2025**, *9*, doi:10.1097/HC9.0000000000000606.
75. Takahashi, Y. Histopathology of Nonalcoholic Fatty Liver Disease/Nonalcoholic Steatohepatitis. *WJG* **2014**, *20*, 15539, doi:10.3748/wjg.v20.i42.15539.
76. Brown, G.T.; Kleiner, D.E. Histopathology of Nonalcoholic Fatty Liver Disease and Nonalcoholic Steatohepatitis. *Metabolism* **2016**, *65*, 1080–1086, doi:10.1016/j.metabol.2015.11.008.
77. Goodman, Z.D. Role of Liver Biopsy in Clinical Trials and Clinical Management of Nonalcoholic Fatty Liver Disease. *Clinics in Liver Disease* **2023**, *27*, 353–362, doi:10.1016/j.cld.2023.01.017.
78. Kim, H.Y.; Rosenthal, S.B.; Liu, X.; Miciano, C.; Hou, X.; Miller, M.; Buchanan, J.; Poirion, O.B.; Chilin-Fuentes, D.; Han, C.; et al. Multi-Modal Analysis of Human Hepatic Stellate Cells Identifies Novel Therapeutic Targets for Metabolic Dysfunction-Associated Steatotic Liver Disease. *Journal of Hepatology* **2025**, *82*, 882–897, doi:10.1016/j.jhep.2024.10.044.
79. Cobelo-Gómez, S.; García-Formoso, L.; Fernández-Pombo, A.; Lázare-Iglesias, H.; Díaz-López, E.; Prado-Moraña, T.; Rodríguez-Sobrino, L.; Senra, A.; Araújo-Vilar, D.; Sánchez-Iglesias, S. Metabolic-Associated Steatotic Liver Disease and FGF21 Dysregulation in Seipin-Deficient and BSCL2-Associated Celia's Encephalopathy Murine Models. *IJMS* **2025**, *26*, 12037, doi:10.3390/ijms262412037.
80. Jeong, B.-K.; Choi, W.-I.; Choi, W.; Moon, J.; Lee, W.H.; Choi, C.; Choi, I.Y.; Lee, S.-H.; Kim, J.K.; Ju, Y.S.; et al. A Male Mouse Model for Metabolic Dysfunction-Associated Steatotic Liver Disease and Hepatocellular Carcinoma. *Nat Commun* **2024**, *15*, 6506, doi:10.1038/s41467-024-50660-y.
81. Bedossa, P. [Presentation of a grid for computer analysis for compilation of histopathologic lesions in chronic viral hepatitis C. Cooperative study of the METAVIR group]. *Ann Pathol* **1993**, *13*, 260–265.
82. Kleiner, D.E.; Brunt, E.M.; Van Natta, M.; Behling, C.; Contos, M.J.; Cummings, O.W.; Ferrell, L.D.; Liu, Y.; Torbenson, M.S.; Unalp-Arida, A.; et al. Design and Validation of a Histological Scoring System for Nonalcoholic Fatty Liver Disease†. *Hepatology* **2005**, *41*, 1313–1321, doi:10.1002/hep.20701.
83. Brunt, E.M.; Janney, C.G.; Di Bisceglie, A.M.; Neuschwander-Tetri, B.A.; Bacon, B.R. Nonalcoholic Steatohepatitis: A Proposal for Grading and Staging The Histological Lesions. *American Journal of Gastroenterology* **1999**, *94*, 2467–2474, doi:10.1111/j.1572-0241.1999.01377.x.
84. Brunt, E.M.; Kleiner, D.E.; Wilson, L.A.; Belt, P.; Neuschwander-Tetri, B.A. Nonalcoholic Fatty Liver Disease (NAFLD) Activity Score and the Histopathologic Diagnosis in NAFLD: Distinct Clinicopathologic Meanings §Δ. *Hepatology* **2011**, *53*, 810–820, doi:10.1002/hep.24127.

 doi:10.20944/preprints202602.1274.v1

85. Bedossa, P.; Poitou, C.; Veyrie, N.; Bouillot, J.-L.; Basdevant, A.; Paradis, V.; Tordjman, J.; Clement, K. Histopathological Algorithm and Scoring System for Evaluation of Liver Lesions in Morbidly Obese Patients. *Hepatology* **2012**, *56*, 1751–1759, doi:10.1002/hep.25889.
86. Liang, W.; Menke, A.L.; Driessen, A.; Koek, G.H.; Lindeman, J.H.; Stoop, R.; Havekes, L.M.; Kleemann, R.; Van Den Hoek, A.M. Establishment of a General NAFLD Scoring System for Rodent Models and Comparison to Human Liver Pathology. *PLoS ONE* **2014**, *9*, e115922, doi:10.1371/journal.pone.0115922.
87. Liss, K.H.H.; McCommis, K.S.; Chambers, K.T.; Pietka, T.A.; Schweitzer, G.G.; Park, S.L.; Nalbantoglu, I.; Weinheimer, C.J.; Hall, A.M.; Finck, B.N. The Impact of Diet-induced Hepatic Steatosis in a Murine Model of Hepatic Ischemia/Reperfusion Injury. *Liver Transpl* **2018**, *24*, 908–921, doi:10.1002/lt.25189.
88. Yan, M.; Cui, Y.; Xiang, Q. Metabolism of Hepatic Stellate Cells in Chronic Liver Diseases: Emerging Molecular and Therapeutic Interventions. *Theranostics* **2025**, *15*, 1715–1740, doi:10.7150/thno.106597.
89. Yashaswini, C.N.; Qin, T.; Bhattacharya, D.; Amor, C.; Lowe, S.; Lujambio, A.; Wang, S.; Friedman, S.L. Phenotypes and Ontogeny of Senescent Hepatic Stellate Cells in Metabolic Dysfunction-Associated Steatohepatitis. *Journal of Hepatology* **2024**, *81*, 207–217, doi:10.1016/j.jhep.2024.03.014.
90. Ramachandran, P.; Brice, M.; Sutherland, E.F.; Hoy, A.M.; Papachristoforou, E.; Jia, L.; Turner, F.; Kendall, T.J.; Marwick, J.A.; Carragher, N.O.; et al. Aberrant Basement Membrane Production by HSCs in MASLD Is Attenuated by the Bile Acid Analog INT-767. *Hepatology Communications* **2024**, *8*, doi:10.1097/HC9.0000000000000574.
91. Wattacheril, J.J.; Abdelmalek, M.F.; Lim, J.K.; Sanyal, A.J. AGA Clinical Practice Update on the Role of Noninvasive Biomarkers in the Evaluation and Management of Nonalcoholic Fatty Liver Disease: Expert Review. *Gastroenterology* **2023**, *165*, 1080–1088, doi:10.1053/j.gastro.2023.06.013.
92. Neuberger, J.; Patel, J.; Caldwell, H.; Davies, S.; Hebditch, V.; Hollywood, C.; Hubscher, S.; Karkhanis, S.; Lester, W.; Roslund, N.; et al. Guidelines on the Use of Liver Biopsy in Clinical Practice from the British Society of Gastroenterology, the Royal College of Radiologists and the Royal College of Pathology. *Gut* **2020**, *69*, 1382–1403, doi:10.1136/gutjnl-2020-321299.
93. Bassegoda, O.; Olivas, P.; Turco, L.; Mandorfer, M.; Serra-Burriel, M.; Tellez, L.; Kwanten, W.; Laroyenne, A.; Farcau, O.; Alvarado, E.; et al. Decompensation in Advanced Nonalcoholic Fatty Liver Disease May Occur at Lower Hepatic Venous Pressure Gradient Levels Than in Patients With Viral Disease. *Clin Gastroenterol Hepatol* **2022**, *20*, 2276-2286.e6, doi:10.1016/j.cgh.2021.10.023.
94. Aggarwal, S.N.; Magdaleno, T.; Klocksieben, F.; MacFarlan, J.E.; Goonewardene, S.; Zator, Z.; Shah, S.; Shah, H.N. A Prospective, Head-to-Head Comparison of 2 EUS-Guided Liver Biopsy Needles in Vivo. *Gastrointestinal Endoscopy* **2021**, *93*, 1133–1138, doi:10.1016/j.gie.2020.09.050.
95. Cassidy, F.H.; Yokoo, T.; Aganovic, L.; Hanna, R.F.; Bydder, M.; Middleton, M.S.; Hamilton, G.; Chavez, A.D.; Schwimmer, J.B.; Sirlin, C.B. Fatty Liver Disease: MR Imaging Techniques for the Detection and Quantification of Liver Steatosis. *Radiographics* **2009**, *29*, 231–260, doi:10.1148/rg.291075123.
96. Pineda, N.; Sharma, P.; Xu, Q.; Hu, X.; Vos, M.; Martin, D.R. Measurement of Hepatic Lipid: High-Speed T2-Corrected Multiecho Acquisition at^{1} H MR Spectroscopy—A Rapid and Accurate Technique. *Radiology* **2009**, *252*, 568–576, doi:10.1148/radiol.2523082084.
97. Heinemann, F.; Gross, P.; Zeveleva, S.; Qian, H.S.; Hill, J.; Höfer, A.; Jonigk, D.; Diehl, A.M.; Abdelmalek, M.; Lenter, M.C.; et al. Deep Learning-Based Quantification of NAFLD/NASH Progression in Human Liver Biopsies. *Sci Rep* **2022**, *12*, 19236, doi:10.1038/s41598-022-23905-3.
98. Huang, Q.; Qadri, S.F.; Bian, H.; Yi, X.; Lin, C.; Yang, X.; Zhu, X.; Lin, H.; Yan, H.; Chang, X.; et al. A Metabolome-Derived Score Predicts Metabolic Dysfunction-Associated Steatohepatitis and Mortality from Liver Disease. *Journal of Hepatology* **2025**, *82*, 781–793, doi:10.1016/j.jhep.2024.10.015.
99. Frączek, J.; Sowa, A.; Agopsowicz, P.; Migacz, M.; Dylińska-Kala, K.; Holecki, M. Non-Invasive Tests as a Replacement for Liver Biopsy in the Assessment of MASLD. *Medicina* **2025**, *61*, 736, doi:10.3390/medicina61040736.
100. Aggarwal, P.; Alkhouri, N. Artificial Intelligence in Nonalcoholic Fatty Liver Disease: A New Frontier in Diagnosis and Treatment. *Clinical Liver Disease* **2021**, *17*, 392–397, doi:10.1002/cld.1071.

 doi:10.20944/preprints202602.1274.v1

101. Goh, G.B.-B.; Leow, W.Q.; Liang, S.; Wan, W.K.; Lim, T.K.H.; Tan, C.K.; Chang, P.E. Quantification of Hepatic Steatosis in Chronic Liver Disease Using Novel Automated Method of Second Harmonic Generation and Two-Photon Excited Fluorescence. *Sci Rep* **2019**, *9*, 2975, doi:10.1038/s41598-019-39783-1.
102. Ferraioli, G.; Barr, R.G.; Berzigotti, A.; Sporea, I.; Wong, V.W.-S.; Reiberger, T.; Karlas, T.; Thiele, M.; Cardoso, A.C.; Ayonrinde, O.T.; et al. WFUMB Guidelines/Guidance on Liver Multiparametric Ultrasound. Part 2: Guidance on Liver Fat Quantification. *Ultrasound Med Biol* **2024**, *50*, 1088–1098, doi:10.1016/j.ultrasmedbio.2024.03.014.
103. Yin, H.; Xiong, B.; Yu, J.; Fan, Y.; Zhou, B.; Sun, Y.; Wang, L.; Xu, H.; Zhu, Y. Interoperator Reproducibility of Quantitative Ultrasound Analysis of Hepatic Steatosis in Participants with Suspected MASLD: A Prospective Study. *European Journal of Radiology* **2024**, *175*, 111427, doi:10.1016/j.ejrad.2024.111427.
104. Ferraioli, G.; Monteiro, L.B.S. Ultrasound-Based Techniques for the Diagnosis of Liver Steatosis. *WJG* **2019**, *25*, 6053–6062, doi:10.3748/wjg.v25.i40.6053.
105. Pirmoazen, A.M.; Khurana, A.; El Kaffas, A.; Kamaya, A. Quantitative Ultrasound Approaches for Diagnosis and Monitoring Hepatic Steatosis in Nonalcoholic Fatty Liver Disease. *Theranostics* **2020**, *10*, 4277–4289, doi:10.7150/thno.40249.
106. Starekova, J.; Hernando, D.; Pickhardt, P.J.; Reeder, S.B. Quantification of Liver Fat Content with CT and MRI: State of the Art. *Radiology* **2021**, *301*, 250–262, doi:10.1148/radiol.2021204288.
107. Khalid, W.B.; Farhat, N.; Lavery, L.; Jarnagin, J.; Delany, J.P.; Kim, K. Non-Invasive Assessment of Liver Fat in Ob/Ob Mice Using Ultrasound-Induced Thermal Strain Imaging and Its Correlation with Hepatic Triglyceride Content. *Ultrasound in Medicine & Biology* **2021**, *47*, 1067–1076, doi:10.1016/j.ultrasmedbio.2020.12.014.
108. Sha, T.; You, Y.; Miao, X.; Deng, H.; Zhang, W.; Ye, H.; Wang, P.; Zheng, R.; Ren, J.; Yin, T. Sequential Ultrasound Molecular Imaging for Noninvasive Identification and Assessment of Non-Alcoholic Steatohepatitis in Mouse Models. *Liver Research* **2023**, *7*, 342–351, doi:10.1016/j.livres.2023.11.002.
109. Czernuszewicz, T.J.; Wang, Y.; Jiang, L.; Kim, K.; Mikulski, Z.; Aji, A.M.; Rojas, J.D.; Gessner, R.C.; Schnabl, B. Noninvasive Monitoring of Steatotic Liver Disease in Western Diet-Fed Obese Mice Using Automated Ultrasound and Shear Wave Elastography. *Liver International* **2025**, *45*, e16141, doi:10.1111/liv.16141.
110. Amin, M.N.; Rushdi, M.A.; Marzaban, R.N.; Yosry, A.; Kim, K.; Mahmoud, A.M. Wavelet-Based Computationally-Efficient Computer-Aided Characterization of Liver Steatosis Using Conventional B-Mode Ultrasound Images. *Biomedical Signal Processing and Control* **2019**, *52*, 84–96, doi:10.1016/j.bspc.2019.03.010.
111. De Rosa, L.; L'Abbate, S.; Kusmic, C.; Faita, F. Applications of Deep Learning Algorithms to Ultrasound Imaging Analysis in Preclinical Studies on In Vivo Animals. *Life* **2023**, *13*, 1759, doi:10.3390/life13081759.
112. Wibulpolprasert, P.; Subpinyo, B.; Chirnaksorn, S.; Shantavasinkul, P.C.; Putadechakum, S.; Phongkitkarun, S.; Sritara, C.; Angkathunyakul, N.; Sumritpradit, P. Correlation between Magnetic Resonance Imaging Proton Density Fat Fraction (MRI-PDFF) and Liver Biopsy to Assess Hepatic Steatosis in Obesity. *Sci Rep* **2024**, *14*, 6895, doi:10.1038/s41598-024-57324-3.
113. Jiang, X.; Washington, M.K.; Izzy, M.J.; Piantek, G.; Lu, M.; Yan, X.; Gore, J.C.; Xu, J. Noninvasive Assessment of Liver Inflammation in Metabolic Dysfunction Associated Steatohepatitis Using MR Cytometry. *npj Imaging* **2025**, *3*, 17, doi:10.1038/s44303-025-00080-4.
114. Bohte, A.E.; Koot, B.G.P.; Van Der Baan-Slootweg, O.H.; Rijcken, T.H.P.; Van Werven, J.R.; Bipat, S.; Nederveen, A.J.; Jansen, P.L.M.; Benninga, M.A.; Stoker, J. US Cannot Be Used to Predict the Presence or Severity of Hepatic Steatosis in Severely Obese Adolescents. *Radiology* **2012**, *262*, 327–334, doi:10.1148/radiol.11111094.
115. Lee, S.S.; Park, S.H.; Kim, H.J.; Kim, S.Y.; Kim, M.-Y.; Kim, D.Y.; Suh, D.J.; Kim, K.M.; Bae, M.H.; Lee, J.Y.; et al. Non-Invasive Assessment of Hepatic Steatosis: Prospective Comparison of the Accuracy of Imaging Examinations. *Journal of Hepatology* **2010**, *52*, 579–585, doi:10.1016/j.jhep.2010.01.008.
116. Van Werven, J.R.; Marsman, H.A.; Nederveen, A.J.; Smits, N.J.; Ten Kate, F.J.; Van Gulik, T.M.; Stoker, J. Assessment of Hepatic Steatosis in Patients Undergoing Liver Resection: Comparison of US, CT, T1-Weighted Dual-Echo MR Imaging, and Point-Resolved^{1}H MR Spectroscopy. *Radiology* **2010**, *256*, 159–168, doi:10.1148/radiol.10091790.

 doi:10.20944/preprints202602.1274.v1

117. Xavier, A.; Zacconi, F.; Santana-Romo, F.; Eykyn, T.R.; Lavin, B.; Phinikaridou, A.; Botnar, R.; Uribe, S.; Oyarzún, J.E.; Cabrera, D.; et al. Assessment of Hepatic Fatty Acids during Non-Alcoholic Steatohepatitis Progression Using Magnetic Resonance Spectroscopy. *Annals of Hepatology* **2021**, *25*, 100358, doi:10.1016/j.aohep.2021.100358.
118. Waghorn, P.A.; Ferreira, D.S.; Erstad, D.J.; Rotile, N.J.; Masia, R.; Jones, C.M.; Tu, C.; Sojoodi, M.; Chen, Y.I.; Schlerman, F.; et al. Quantitative, Noninvasive MRI Characterization of Disease Progression in a Mouse Model of Non-Alcoholic Steatohepatitis. *Sci Rep* **2021**, *11*, 6105, doi:10.1038/s41598-021-85679-4.
119. Tang, H.; Li, J.; Zinker, B.; Boehm, S.; Mauer, A.; Rex-Rabe, S.; Glaser, K.J.; Fronheiser, M.; Bradstreet, T.; Nakao, Y.; et al. Evaluation of a PEGylated Fibroblast Growth Factor 21 Variant Using Novel Preclinical Magnetic Resonance Imaging and Magnetic Resonance Elastography in a Mouse Model of Nonalcoholic Steatohepatitis. *Magnetic Resonance Imaging* **2022**, *56*, 712–724, doi:10.1002/jmri.28077.
120. Xia, H.; Min, Y.; Wang, Y.; Gao, S.; Wang, H.; Yan, F.; Liu, R.; Wang, J.; Gu, X.; Bo, T. Multiparametric MRI Evaluation of Liver Fat and Iron after Glucagon-like Peptide-1 Receptor and Glucagon Receptor Dual-Agonist Treatment in a High-Fat Diet–Induced Mouse Model. *Radiology* **2025**, *316*, e243780, doi:10.1148/radiol.243780.
121. Lavin, B.; Eykyn, T.R.; Phinikaridou, A.; Xavier, A.; Kumar, S.; Buqué, X.; Aspichueta, P.; Sing-Long, C.; Arrese, M.; Botnar, R.M.; et al. Characterization of Hepatic Fatty Acids Using Magnetic Resonance Spectroscopy for the Assessment of Treatment Response to Metformin in an eNOS$^{-/-}$ Mouse Model of Metabolic Nonalcoholic Fatty Liver Disease/Nonalcoholic Steatohepatitis. *NMR in Biomedicine* **2023**, *36*, e4932, doi:10.1002/nbm.4932.
122. Lister, D.; Blizard, G.; Hosseini, M.; Messer, K.; Wellen, J.; Sirlin, C.B.; Ahrens, E.T. Imaging Non-Alcoholic Fatty Liver Disease Model Using H-1 and F-19 MRI. *Mol Imaging Biol* **2023**, *25*, 443–449, doi:10.1007/s11307-022-01798-y.
123. McLeod, M.; Chang, M.C.; Rushin, A.; Ragavan, M.; Mahar, R.; Sharma, G.; Badar, A.; Giacalone, A.; Glanz, M.E.; Malut, V.R.; et al. Detecting Altered Hepatic Lipid Oxidation by MRI in an Animal Model of MASLD. *Cell Reports Medicine* **2024**, *5*, 101714, doi:10.1016/j.xcrm.2024.101714.